

Palynology and climate change of the Norian at Petrified Forest National Park, Arizona

Tammo Reichgelt



Research project at Utrecht University, Biogeology Master Program, Institute of Environmental Biology, Palaeo-ecology Group

Utrecht University, Department of Biology supervisors:
Dr. Wolfram M. Kürschner
Prof. Dr. Johanna H.A. van Konijnenburg-van Cittert

Utrecht University, Department of Geology supervisor:
Dr. Wilma Wessels

Petrified Forest National Park supervisors:
William G. Parker
Dr. Jeffrey W. Martz

Table of Contents

Abstract	5
Introduction	6
Study Area & Lithology	6
Introduction Chinle Formation at Petrified Forest National Park	6
Introduction Sonsela Member	7
Sampling strategy and significant beds of the Sonsela Member	8
Materials & Methods	10
Palynology.....	10
Cuticular analysis	10
Organic carbon isotope analysis	11
Systematic palynology	11
General introduction systematic palynology	11
Sulcate bisaccate pollen.....	12
Taeniate bisaccate pollen.....	13
Other bisaccate pollen	13
Trilete monosaccate pollen.....	17
Other monosaccate pollen	17
Monosulcate pollen	18
Spores	18
Palaeobotanical affinities	20
Importance and methods assigning palaeobotanical affinities	20
Coniferous pollen types.....	21
Other Gymnospermous pollen types	22
Spore producing plant types	22
Results	23
Palynoflora	23
Cuticula	25
$\delta^{13}\text{C}_{\text{TOC}}$ and total organic carbon percentage.....	25
PCA	26
Discussion	26
Palaeo-environment.....	26
Fauna change – Flora change	27
$\delta^{13}\text{C}_{\text{TOC}}$ and total organic carbon percentage.....	32

Principal Components Analysis	34
Assessing possible causes.....	36
Conclusions and Future Research	37
Conclusions	37
Future Research	38
Acknowledgements	38
References	38
APPENDIX A	43
APPENDIX B.....	50
APPENDIX C	52

Table of Figures and Tables

Figure 1: Outcrops Chinle Formation and map Petrified Forest National Park	7
Figure 2: General lithology Chinle Formation at Petrified Forest National Park.....	8
Figure 3: Lithologs relevant sections	9
Figure 4: Lithology Sonsela Member and sectioned intervals	10
Table 1: Botanical affinities important palynomorphs	20
Figure 5: Relative species abundances	24
Figure 6: $\delta^{13}\text{C}_{\text{TOC}}$ and total organic carbon percentage	25
Figure 7: PCA analysis	26
Figure 8: Pie chart overall plant type percentages.....	27
Figure 9: Relative abundances plant types	28
Figure 10: Relative species abundances with $\delta^{13}\text{C}_{\text{TOC}}$ and zonation	30
Figure 11: Different morphotypes <i>Klausipollenites gouldii</i>	31
Figure 12: Relative abundance xenomorphs and <i>Froelichsporites traversei</i>	31
Figure 13a: $\delta^{13}\text{C}_{\text{TOC}}$ vs. TOC (%) all samples	33
Figure 13b: $\delta^{13}\text{C}_{\text{TOC}}$ vs. TOC (%) high organic carbon percentage.....	33
Figure 13c: $\delta^{13}\text{C}_{\text{TOC}}$ vs. TOC (%) low organic carbon percentage	33
Figure 14: $\delta^{13}\text{C}_{\text{TOC}}$ of Badlands and Devil's Playground sections	34
Figure 15: PCA with important plant groups	35

Abstract

The late Triassic is characterized by several pulses of biotic turnover, both regional and global, before the end-Rhaetian mass extinction. The development of a solid lithostratigraphic framework of the continental sandstones and mudstones at Petrified Forest National Park revealed that a faunal turnover took place within the Norian stage of the Chinle Formation.

With an uncertainty of ~2.3 meters from the interval of faunal turnover, the abundance of Pteridosperm and Palaeozoic Conifer pollen types decline. Overall diversity drops at this interval, whereas the alleged Mesozoic Conifer pollen species *Klausipollenites gouldii* becomes dominant, at some point comprising over 50% of the assemblage. There is a short lived spike in spore taxa and some other pollen taxa. These taxa can be associated with an increased supply of moisture and/or a short decline in light intensity, as ferns are known to thrive under low light. Following the spike in spore taxa, *K. gouldii* stays dominant, but other taxa, which declined at the faunal turnover, increase in abundance again.

The occurrence of xenomorphic structures in *Klausipollenites gouldii* can be interpreted as signals for environmental deterioration. There is a large increase in xenomorphic structures in *K. gouldii* at the same interval where the spore taxa occur and after both the xenomorphic structures and the post disaster taxa are on the decline again, the tetrahedral tetrad *Froelichsporites traversei* increases in abundance. The occurrence of the enigmatic spore taxa *F. traversei* could be indicative of continued drought or environmental stress.

Measurements on $\delta^{13}\text{C}_{\text{TOC}}$ throughout the interval show large fluctuations through the entire section. Ideally this could be attributed to fluctuations in the moisture supply at the interval, although this also could be a local anomaly, or to fluctuations in the stable isotope values of atmospheric CO_2 . However, it is a possibility that these fluctuations are the result of variable sediment types, as the total organic carbon percentage varies from 0.01% in claystone deposits, to 35% in highly coalified plant beds.

There are some signatures here of a short biotic perturbation, causing local or regional flora to change. The increased spore taxa suggest that moisture supply and/or light intensity played a role in this. The increase of xenomorphic structures and the disappearance and/or decline of multiple pollen taxa suggest that environmental circumstances deteriorated; this implies that changes in the moisture supply was not the only environmental component affected.

It remains to be investigated what the cause of this turnover was, which occurs in a relatively short time span and if the turnover only occurs locally or in more sections throughout North America. There is a very rough correspondence between the dating of the Manicouagan impact in eastern Canada and the change occurring at Petrified Forest National Park. However, there is a lack of datable sections at Petrified Forest National Park to investigate if this could actually be the trigger for this turnover.

Introduction

The end-Triassic extinction marks one of the big five extinctions of the Phanerozoic. It is however likely that the late Triassic witnessed more regional or even global extinctions besides the latest Rhaetian extinction (e.g. Benton, 1986; Sephton et al., 2002). The reasons for these other late Triassic extinctions remain obscure (e.g. Hodych and Dunning, 1992; Walkden et al., 2002; Tanner et al., 2004), except for a general consensus towards the reason of the latest Triassic extinction, being massive outgassing in the area of the Central Atlantic due to the rifting apart of Pangaea (Hesselbo et al., 2002; Marzoli et al., 1999) and consequently methane hydrate release, further destabilizing the climate (Ruhl et al., in prep.).

The Chinle Formation in southwest USA was deposited in the late Triassic, probably ranging from early Norian to Rhaetian (Riggs et al., 2003), not including the Triassic-Jurassic boundary. The Chinle Formation follows the Moenkopi Formation and is followed by the Moenave Formation. Tetrapod fauna's and biostratigraphy of the Chinle Formation have been extensively researched (e.g. Murry and Long, 1989; Parker, 2006). Recently, extensive reviewing of the exposures of the Chinle Formation at Petrified Forest National Park yielded a stratigraphic succession, which seems to solve the problems researchers were formerly confronted with when investigating Chinle Formation geology (Martz and Parker, 2010). Moreover, the stratigraphic revisions of the Chinle Formation elucidated the local tetrapod biostratigraphy, where it now seems that a faunal turnover occurred in the Sonsela member of the Chinle Formation (Parker and Martz, in press.). This faunal turnover roughly coincides with a palynofloral change (Litwin et al., 1991). However, this change is not as well constrained stratigraphically as the found faunal change.

The depositional environment of the Chinle Formation has long been under discussion, most likely it was a highly seasonal semi-arid environment (Cleveland et al., 2008; Dubiel et al., 1991). The general trend of the climate throughout the Chinle Formation was aridification (Prochnow et al., 2006). The riparian lowlands during the time of deposition were dominated by Bennettitales, sphenopsids, Cycadales, pteridophytes and pteridosperms (Ash, 1980; Demko et al., 1998) whereas the upland vegetation was dominated by drought tolerant conifers (Ash, 1999).

By constraining the biostratigraphic interval of faunal turnover geologically at Petrified Forest National Park, it is now possible to investigate whether this faunal turnover coincides with a floral turnover, by investigating palynology at the interval. In this study we investigate whether a floral turnover did occur at the proposed interval of the faunal turnover. Furthermore we present environmental proxies, such as $\delta^{13}\text{C}_{\text{TOC}}$ and the abundance of xenomorphic pollen types, to shed light on the climatic factors playing a role in this turnover.

Study area & Lithology

Introduction Chinle Formation at Petrified Forest National Park

At Petrified Forest National Park a total of ~350 meters of successive outcrop of the Chinle Formation is exposed, ranging from early Norian to middle Rhaetian (Furin et al., 2006; Riggs et al., 2003). The Chinle Formation outcrops in several states in the southwestern USA; Arizona: New Mexico, Utah, Colorado and Nevada. Whereas outcrops of the same age in eastern New Mexico, Texas and Oklahoma are assigned to the Dockum Group and outcrops in southwest Colorado to the Dolores Formation (fig 1). Petrified Forest National Park is located in northeast Arizona at ~35.06N, -109.78W. The exposed outcrops at Petrified Forest

National Park are a variety of grey to white sandstones and a rainbow of mudstones. The petrified logs of which the park is known for are localized in the sandstones. The logs are either completely replaced by silicate crystals or are permineralized in their original structure. The park is rich in vertebrate fossils, especially in the lower members (Mesa Redondo, Blue Mesa and the lower part of the Sonsela Member). These members are also usually of darker color, whereas the upper members (upper Sonsela, Petrified Forest and Owl Rock Member) are usually red and purple and are not as rich in vertebrate fossils. Figure 2 shows the general lithology of the exposed outcrops of the Chinle Formation at Petrified Forest National Park.

Recent revisions of the Carnian and Norian stages place the base of the Norian at a much lower stratigraphic interval (Muttoni et al., 2004; Furin et al., 2006), which places the largest part of the Chinle Formation within the Norian (Riggs et al., 2003; Martz and Parker, 2010). The Carnian-Norian boundary does not outcrop at Petrified Forest National Park and the Norian-Rhaetian boundary most probably occurs near the base of the Owl Rock Member (Martz and Parker, 2010).

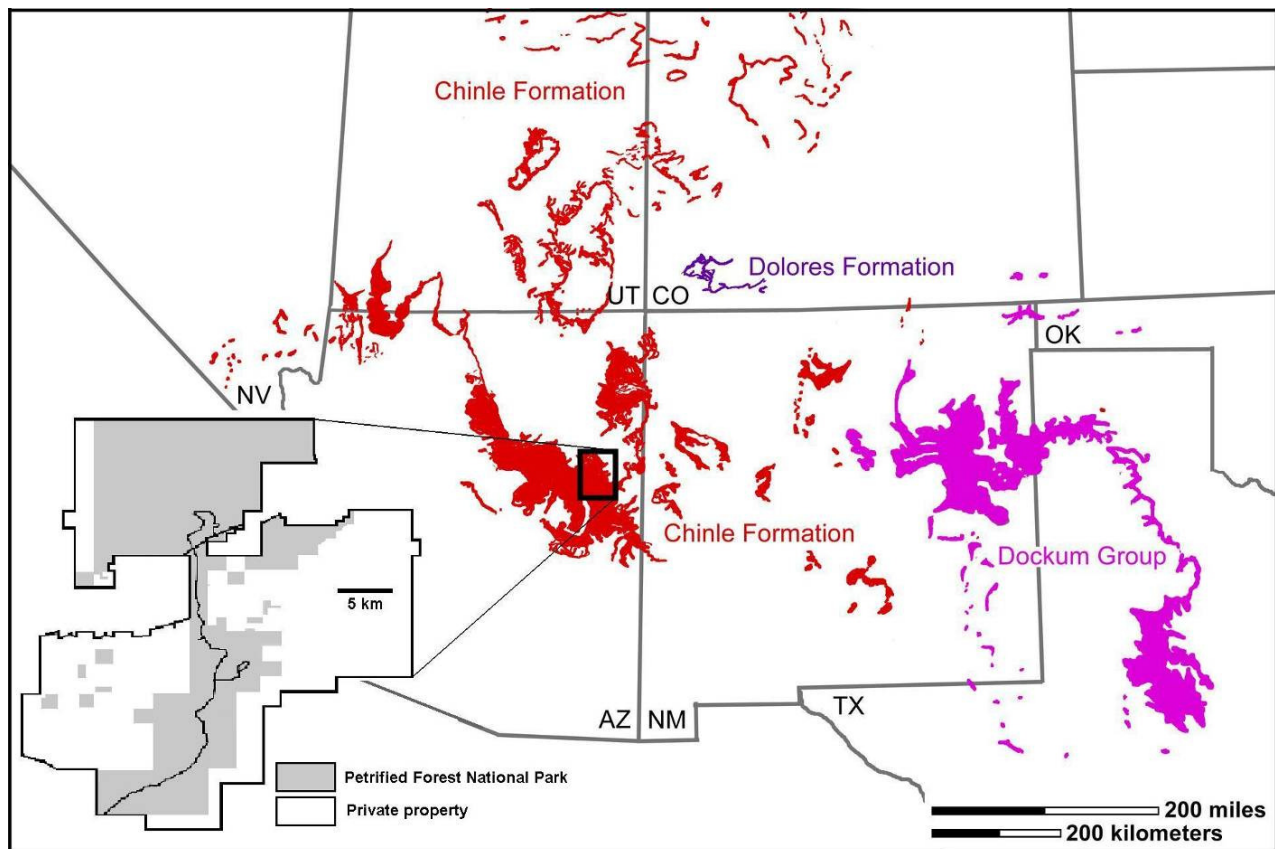


Figure 1: Late Triassic outcrops of Southwestern USA and location of Petrified Forest National Park in respect to these outcrops. Edited from J.W. Martz in Martz and Parker (2010).

Introduction Sonsela Member

The Sonsela Member is the lithological member in which the change in vertebrate fauna occurs (Parker and Martz, in prep.). The Sonsela Member is rich in white and grey sandstone and also contains the richest petrified wood beds: the Jasper Forest Bed (Parker, pers. comm.). The sandstones are interbedded with grey mudstones, which are occasionally rich in plant fossils. There are no notable changes within the Sonsela Member, however ascending into the Petrified Forest Member and the Owl Rock Member sandstones become rarer as do grey

mudstones (Martz and Parker, 2010). The Sonsela Member was formerly not recognized as a member, but as a continuous sandstone body within the Petrified Forest Member (e.g. Murry, 1990). It was first recognized as a separate member by Heckert and Lucas (2002).

For palynological research the sandstones of the Sonsela Member are not ideal. However, large sections of unoxidized mudstone within the Sonsela Member provide excellent material for both palaeobotanical and palynofloral investigations, whereas the sandstone bodies provide excellent stratigraphic marker beds. As there are not many continuous sections at Petrified Forest National Park, a solid stratigraphic framework is vital.

Sampling strategy and significant beds of the Sonsela Member

For palynological investigation the sediment ideally needs to be of a very low grain size and unoxidized. If sediment is of a large grain size (e.g. sand), it was deposited under circumstances wherein the transport energy was too high for organic palynomorphs to settle. If sediment is oxidized, the organic matter within the sediment has been decomposed. This can happen shortly after deposition, if the sediment is exposed to oxygen, or long after deposition, when the rock is weathering out. Oxidized sediment can be recognized by its high manganese and/or iron content, which will make the sediment color purple or red. The most probable depositional environments in the continental deposits of the Chinle Formation are poorly mixed or eutrophic lakes, swamp pools, oxbow lakes or settling pools of water, cut off from rivers.

Samples were collected from continuous mudstone sections, coalified plant beds and other beds which were in association with fossil plant material. The sediments were checked for signs of oxidation (red and purple colors) and thus judged if useful for palynological investigation.

Several outcrops were sampled to create a more or less continuous succession of palynological samples. The Sonsela Member at Petrified Forest National Park (fig 2) is composed of several beds, which are laterally continuous throughout the park. The earlier described faunal turnover occurs just above the Jasper Forest Bed, in the Jim Camp Wash Beds.

1. The stratigraphically lowest section sampled of the Sonsela Member is the Mountain Lion Cliff section, which exposes the Lot's Wife Beds below the Jasper Forest Bed up to the lower part of the Jim Camp Wash Beds above the Jasper Forest Bed. At the Mountain Lion

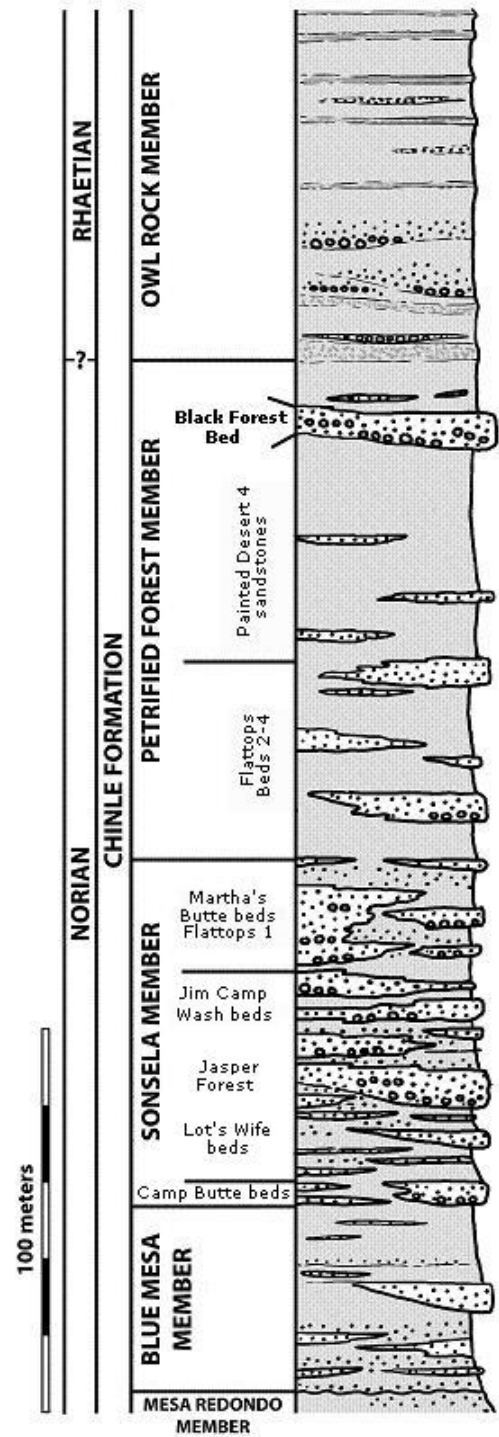


Figure 2: General lithology of the exposed outcrops of the Chinle Formation at Petrified Forest National Park. Courtesy of J.W. Martz

Cliff section there is a thin layer of mudstone which can be found within the Jasper Forest Bed (fig 3).

2. The Devil's Playground section was sampled at an interval where a coalified plant bed was exposed. It is stratigraphically equal to the lower Jim Camp Wash Beds, just above the Kellogg Butte Bed, which is stratigraphically equal to the Jasper Forest Bed (fig 3). The plant bed was 1,5 meters thick and embedded between the Kellogg Butte sandstone and a heavily oxidized mudstone. This bed is of high importance because of the stratigraphic position of the bed relative to the faunal turnover.

3. The Badlands section exposes an outcrop of a coalified plant bed high in the Jim Camp Wash Beds (fig 3).

4. The Mountain Lion Mesa section exposes outcrops from the highest strata of the Jim Camp Wash Beds, starting right above a more or less persistent sandstone layer in this area of the park, called the Mountain Lion sandstone. The Mountain Lion sandstone is locally useful as a stratigraphic marker bed. The section continues right up to the base of the Martha's Butte Beds (fig 3).

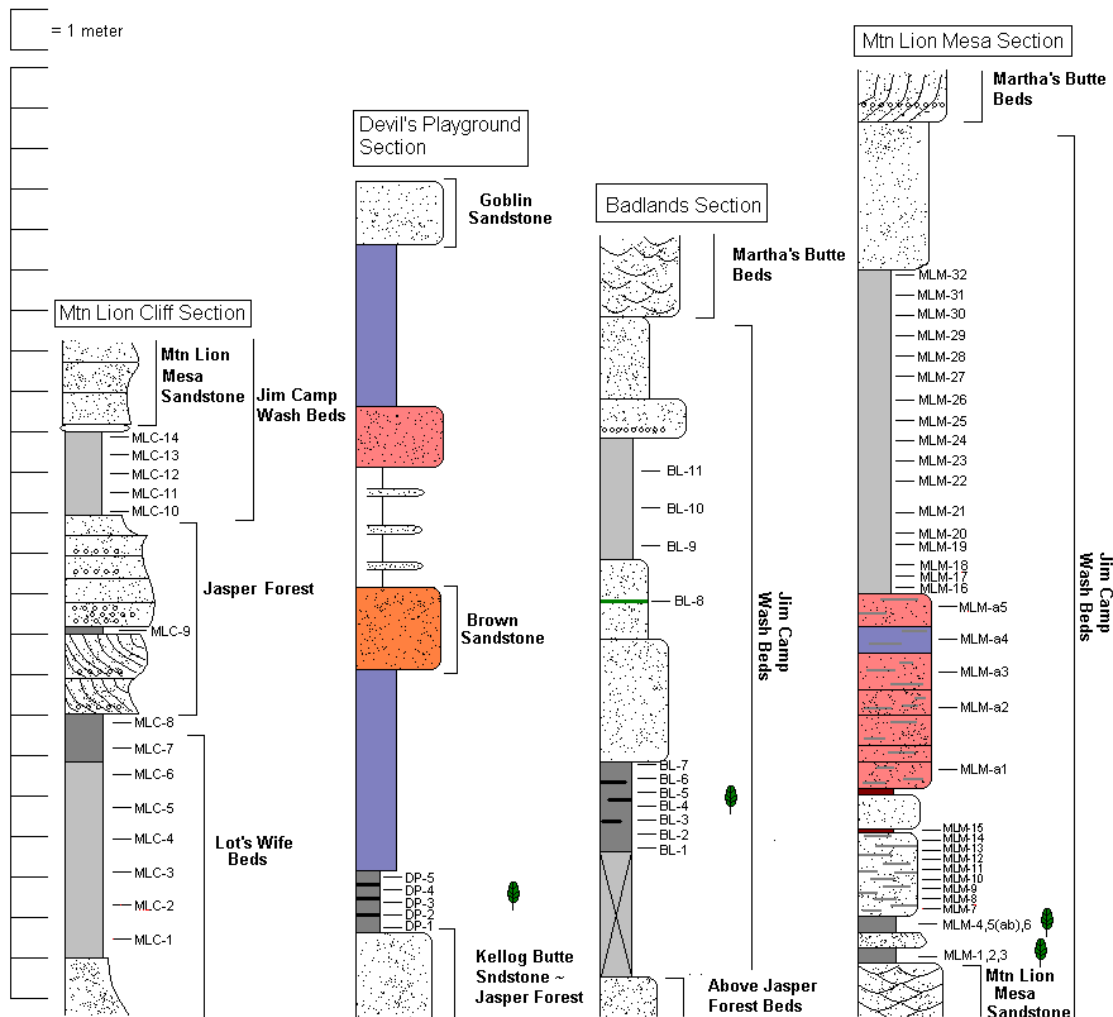


Figure 3: Lithologies of the relevant sampled sections and the relevant beds they occur in.

Materials & Methods

Palynology

At Petrified Forest National Park 77 samples were collected and processed for palynological analysis. Of these samples 15 were productive. The samples all fall within the Sonsela Member of the Chinle Formation, ranging from the upper Lot's Wife Beds to the upper Jim Camp Wash Beds. The average sampling interval was about 30 cm. The samples were collected from different sections within the park. The lithostratigraphic framework of the park was used to estimate overlaps and hiatuses between the different sections (fig 4). The productive samples were from the Devil's Playground section (DP 1-5), the Badlands section (BL 1-7) and the Mountain Lion Mesa section (MLM 1-3).

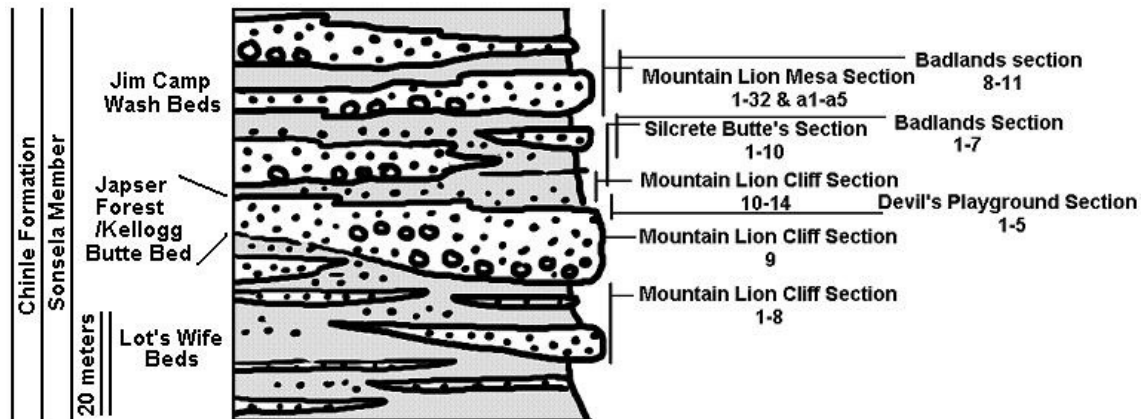


Figure 4: Cropped part of general lithology of Sonsela Member, with sectioned intervals. Abbreviations for sampled sections: Badlands section BL, Mountain Lion Mesa section MLM, Silcrete Butte's section SLC, Mountain Lion Cliff section MLC and Devil's Playground section DP.

From each sample, between 10 and 30 grams of sediment (depending on the type of sediment) were crushed and dried for 24 hours at 60°C. A tablet containing *Lycopodium* spores was added to each sample. All samples were treated alternately with 10% and 30% HCl to remove all carbonates and 40% HF to remove all silicates. The residues were sieved with a mesh of 250µm and 15µm and treated with ZnCl₂ to separate the heavy minerals from the organic material. The heavy minerals were removed and the organic material was again sieved with a mesh of 15 µm. After this slides were made, where the organic material of every sample was mounted on two object glasses using glycerine jelly.

In each sample at least 300 pollen and spores were identified using descriptions and derivations by Nilsson (1958), Jansonius (1962), Mädler (1964), Visscher (1966), Schultz (1967), Dolby and Balme (1976), Dunay and Fisher (1979) and Fisher and Dunay (1984), save the *Lycopodium* spores, which were used to calculate absolute abundances.

Relative abundances were calculated and plotted using the programs Tilia and TgView. The program C2 was used to perform a Principal Components Analysis (PCA). The components of the PCA were normalized to correct for overdominance of a specific component.

Cuticular analysis

11 samples from Petrified Forest National Park samples were found useful for the study of plant debris. The beds at the Badlands and Devil's Playground localities were very rich in coalified leaf debris. The samples BL 2-7 and DP 1-5 (fig 4) of which plant debris was

separated with the 250 μ m sieve were used. After separation the samples were treated with HNO₃, to clean the cuticula. This did not give a strong reaction, also not when the samples were left for 24 hours in a heater at 40°C. Subsequently, Schulze's Reagent was used to clean the cuticula. KClO₃ crystals were partly dissolved in 30% HNO₃, after which the samples were treated with the mixture. The samples were again left for 24 hours in a heater at 40°C. The reaction was then stopped by adding 5% KOH. After this the samples were washed several times with water. Large leaf fragments were picked and mounted on object glasses using glycerine jelly. The method of cuticula laceration was derived from Kerp (1990).

The cuticular fragments were determined on varying taxonomic levels. Some were determined on genus level, others could not be determined any better than on the level of the order.

Organic carbon-isotope analysis

Of 28 samples from Petrified Forest National Park the organic carbon-isotope value was measured. This included samples MLC 1-9, 11 & 14, MLM 1, 3, 4, 7, 10, 13, a5, 16, 17 & 19, BL 1, 3, 5, 7 and DP 1, 3, 5 (fig 4). These samples were chosen because they span a representative selection throughout the section. The samples were pulverized and freeze-dried, before ~1 gram of each sample was treated twice with 15ml cold 1M HCl. These steps were taken to remove all non organic carbon that might obscure the results. After the HCl treatment the samples were rinsed with water free from any minerals and centrifuged (with 2800 rotations per minute, for 15 minutes), until a neutral pH was reached. After freeze-drying the samples again, the samples were weighed to determine the weight loss and thus determining the bulk weight percentages of the carbonates in the samples.

The carbon and nitrogen content of the samples were measured by using a CNS-analyzer on ~9mg of homogenized de-carbonated sample residue. These measurements were performed at the integrated laboratory of the Faculty of Geosciences (Utrecht University). With the TOC values of these samples we were able to determine the bulk weight of the organic carbon in the samples and after this we accurately determined the isotope ratios of the organic carbon in the samples (with a standard deviation of 0.037‰), by Elemental Analyzer Continuous Flow Isotope Ratio Mass Spectrometry using a Fisons 1500 NCS Elemental Analyzer coupled to a Finnigan Mat Delta Plus mass spectrometer at the Geochemistry group of the Department of Earth Sciences (Utrecht University).

Systematic palynology

General introduction systematic palynology

The importance of systematic palynology is often underestimated. Inaccurate descriptions and random appliance of taxonomic names can make it difficult to be consistent in determining ones palynomorphs. Therefore tracing down the original description of a palynomorph is important. This can make a difference in the palaeobotanical affinity of the palynomorph and can lead to a different palaeoecological reconstruction.

Previous palynological studies of the upper Triassic of the American southwest have shown an overall dominance in the palynofacies of the Chinle Formation of bisaccate pollen grains, both in abundance and diversity (e.g. Dunay and Fisher, 1979; Fisher and Dunay, 1984; Litwin et al., 1991). The main focus of systematic palynology in this study will be on bisaccate pollen grains, because we consider the high diversity of bisaccate pollen grains to be of the important in reconstructing the palaeo-environment.

Descriptions of palynomorphs are derived directly from the provided references.

Sulcate bisaccate pollen

Alisporites opii (Daugherty, 1941)

Appendix A: Plate 7, specimen 1

The spores are large, averaging 100 to 110 microns in length and having two large membranaceous wings with reticulate markings. They are spherical to ovate in dorsal view, having a rather thick exine and a single fusiform furrow.

Angustisaccus reniformis (Fisher and Dunay, 1984)

Appendix A: Plate 4, specimen 5

Alete bisaccate pollen: outline haploxytonoid; somewhat kidney shaped. Corpus almost circular in outline; corpus exine punctate, up to 3 μm thick. Distal area of thin exine between sacci but no clearly defined tenuitas. Sacci small, less than $\frac{1}{4}$ of corpus size; distally attached and pendent. Saccus bases well defined forming a narrow ellipse. Sacci densely and finely infrareticulate.

Equatorial diameter: 67-79 μm

Corpus: 61-72 μm

The genus *Angustisaccus* was erected to include bisaccate pollen with transversely elongate sacci with narrow bases which are attached on the distal side of the grain and which border a well defined elongate oval leptoma (Fisher and Dunay, 1984). It was formerly thought to be a type of *Podosporites*.

Protodiploxypinus americus (Dunay and Fisher, 1979)

Appendix A: Plate 4, specimen 1

Alete bisaccate grain, corpus circular to elliptical with the longitudinal axis greater than the transverse axis. Corpus exine double-layered and tectate; sculpture infrareticulate. Sacci semi-circular, always smaller than the corpus, infrarugulate and diaphanous; breadth of sacci $\frac{1}{2}$ to $\frac{2}{3}$ diameter of the corpus. Sacci proximally attached subequatorially and distally pendent; distal saccus bases straight. A sharply delimited, prominent lens-shaped sulcus is present on the distal face of the corpus and extends the full height of the corpus; the greatest width being $\frac{1}{8}$ to $\frac{1}{3}$ of the corpus diameter.

Equatorial diameter: 28-39 μm

Corpus: 20-27 μm

Schizosaccus keuperi (Mädler, 1964)

Appendix A: Plate 5, specimen 3

The corpus is almost spherical to oval, distally frequently somewhat inclined. The clear distal split can reach the equator. The exine is on all sides up to 3 μm thick and infrapunctate. The above the equator attached relatively small sacci are distally striated and above the equatorial end of the sulcus connected by an isolated shaft, which occasionally is deformed and appears to be rolled up. There can also be an isolated shaft through the sulcus-split.

Equatorial diameter: 80-90 μm

Corpus: 50-54 μm

Sulcatisporites kraeuselii (Mädler, 1964)

Appendix A: Plate 6, specimen 2

Bisaccate pollen grain with a round corpus and short, distally attached sacci. The sacci aren't much larger than the corpus, although they envelop the corpus, which causes the circular contour of the whole pollen grain to be preserved. Sacci equatorially attached by a continuous

shaft, distally approaching a small slit. *Sulcatisporites kraeuselii* differs from the type species of *Sulcatisporites* in having reticulated sacci.

Equatorial diameter: 75-90 μm

Taeniate bisaccate pollen

Chordasporites chinleanus (Dunay and Fisher, 1979)

Appendix A: Plate 6, specimen 1

Bisaccate pollen grain. Corpus elliptical, smooth to infrapunctate. On the proximal surface of the corpus up to six 'ribs' may be present, formed by intraexinal differentiation. 'Ribs' 2-4 μm wide, not inflated and faintly developed. Sacci distally pendent, infrarugulate and often equatorially connected by a thin exinal strip; saccus rugae often radially oriented in the region of saccus attachment. Distal germinal aperture is a faint leptoma: no sulcus observed.

Equatorial diameter: 69-90 μm

Corpus diameter: 51-59 μm

The genus *Chordasporites* was erected to include bisaccate pollen with a rib formed by intraexinal thickening, but emended diagnosis assigned pollen grains to this genus with one or several ribs formed by intraexinal thickening (Dunay and Fisher, 1979). The species *Pityosporites chinleanus* was for this reason assigned to *Chordasporites chinleanus*.

Trilete bisaccate pollen

Triadispora dockumensis (Dunay and Fisher, 1979)

Appendix A: Plate 3, specimen 6

Trilete, bilaterally monosaccate, rarely bisaccate pollen grain. Corpus elliptical with transverse axis greater than longitudinal axis; dense, darker than sacci; corpus finely infrarugulate. Trilete mark usually small, indistinct, simple, and offset from the proximal pole. Sacci infrareticulate, filamentous, usually connected equatorially.

Equatorial diameter: 56-85 μm

Corpus: 28-38 μm

Triadispora fallax (Fisher and Dunay, 1984)

Appendix A: Plate 3, specimen 3

Bisaccate trilete pollen, outline diploxytonoid tending towards haploxytonoid. Corpus oval to sub-rounded with longitudinal axis barely greater than transverse axis. Corpus exine without visible surface ornament, but with a poorly defined infrastructure: punctate, 2 μm thick. Sacci slightly smaller than corpus, weakly distally inclined; saccus bases of the indistinct. Sacci finely infrareticulate. On the proximal face there is a small, frequently indistinct trilete mark, the rays of which never exceed 4 μm in length. The distal area is slightly thinner than the remainder of the corpus, but does not possess a well-defined sulcus.

Equatorial diameter: 67-85 μm

Corpus: 41-59 μm

Other bisaccate pollen

Colpectopollis ellipsoideus (Visscher, 1966)

Appendix A: Plate 7, specimen 4

Pollen bisaccate, alete. Elliptical outline both in polar view and in equatorial view; this is due to the original ellipsoid shape of the pollen grain. Equator of the central body approximately circular to longitudinally elliptical. Central body with proximally thickened exine (3-3.5 μm).

Sacci haploxytonoid, equatorially interconnected. Very indistinct distal germinal area which is fundamentally fusiform. Both the thickened proximal exine of the central body and the unthickened distal exine can be longitudinally folded. This happens very frequently and in a very characteristic way.

Known size range: 70-100 μm .

Klausipollenites schaubergeri (Jansonius, 1962)

Appendix A: Plate 6, specimen 4

Bisaccate grains, usually without an Y-mark; sacci show more or less displacement towards distal pole, proximally attached near equator, no sharp delineation of bladder masses; germinal area over distal pole broad, indistinctly defined but general thinner than rest of spore wall; equatorial outline smoothly oval, in equatorial view slightly bean-shaped; bladders in shape varying between crescent and half-circular; proximal exoexine may show some thickening, usually not inflated but in some cases a slight subequatorial inflation interconnecting the bladders.

Equatorial diameter: 40-60 μm

Corpus: 20-30 μm

Klausipollenites gouldii (Dunay and Fisher, 1979)

Appendix A: Plate 3, specimen 5

Alete bisaccate pollen grain; outline usually haploxytonoid. Corpus finely infrareticulate, circular to elliptical with the transverse axis greater than the longitudinal axis. Sacci crescent-shaped, more coarsely infrareticulate than the corpus, proximally attached near the equator, slightly distally pendent. No sharp delineation of saccus bases; sacci occasionally connected by a thin equatorial strip of exine. Distal germinal aperture is a leptoma which is indistinctly defined but possesses a thinner exine than the remainder of the corpus.

Equatorial diameter: 43-56 μm

Corpus: 20-26 μm

Minutosaccus crenulatus (Dolby and Balme, 1976)

Appendix A: Plate 3, specimen 7

Disaccate diploxytonoid pollen grains. Corpus transversely elongate oval or almost circular. Cappa markedly convex, 1-3 μm thick, finely intrareticulate. Sacci distally detached, rounded to sub-triangular, the line of saccus detachment bordering the cappa is straight, slightly curved or irregular, the remainder is detached along an arcuate line close to the margin of the distal surface. In some specimens the sacci are united sub-equatorially to enclose an elongate oval, slightly depressed, thin unstructured, cappa. Sacci coarsely columellate, structural elements radially elongate in compressed specimens and not forming a clearly defined intrareticulum. Surface of sacci radially or irregularly crenulated.

Breadth: 33-56 μm

Corpus: 29-39 μm

Pityosporites devolens (Leschik, 1956)

Appendix A: Plate 5, specimen 2

The contour of the pollen corpus is circular, in equatorial view the corpus is oval to circular. The exine of the corpus is reticulate. The exine is about 1.5 μm thick. The sacci are clearly displaced from the pollen corpus. The sacci have a netted structure of lumina of varying diameter. In general the narrow attachment area dominate, but wide attachment area is present at the distant poles, with a maximum diameter of 3.5 μm and a minimum of 0.5 μm . At the distal pole the attachment area of the saccus can be at a distance up to 8 μm .

Breadth: up to 100 µm
Corpus: up to 60 µm

Plicatisaccus badius (Pautsch, 1973)

Appendix A: Plate 3, specimen 2

Bisaccate pollen grains with thick, brown exine. Body oval, much longer than broad, opaque; structure indistinct, probably infragranulate. In specimens flatly compressed in polar position, the body exine bends and overlaps, giving the impression of a ruff around the body. The breadth of the overlap extends up to 8µm. In equatorial view, body nearly triangular. Bladders brown, with radially disposed rows of reticulum lumina and radial folding of the bladder wall, especially on the distal side. Distal roots not clearly visible, usually crescent-shaped. Often bladders secondarily and centripetally brought together, so that a narrow parallel-sided space is formed distally between them. This space has undulate margins on account of the ridges of radial exine foldings.

Equatorial diameter: 53-73 µm

Corpus: 38-60 µm

Protodiploxylinus ujhelyi (Dunay and Fisher, 1979)

Appendix A: Plate 4, specimen 2

Alete bisaccate grain, corpus circular to elliptical. Exine thin, two-layered, tectate; sculpture faintly infrareticulate. Sacci thin, semi-circular, always smaller than the corpus, finely infrarugulate with individual elements radially oriented. Breadth of sacci ½ to 2/3 corpus diameter. Proximal attachment equatorial; distal saccus bases usually straight. No distinct sulcus is present. Germinal aperture is an ill-defined, broad distal leptoma.

Equatorial diameter: 17-33 µm

Corpus: 15-20 µm

Protodiploxylinus ujhelyi and *Protodiploxylinus americanus* were found in situ with the gymnospermous microsporophyll *Pramelreuthia*, which resembles the microsporophyll of a Bennetitalean. Therefore the botanical affinity of *P. ujhelyi* and *P. americanus* are indicated as Bennetitalean in this study. However, the other species of the genus *Protodiploxylinus*, *P. fastidiosus* and *P. lacertosus*, have not been found in situ with *Pramelreuthia*. It is therefore doubtful if these two species are closely related to Bennetitaleans. In this study we assign all species of *Protodiploxylinus* to the Bennetitaleans, but perhaps a *P. fastidiosus* and *P. lacertosus* need to be assigned to another genus.

Protodiploxylinus lacertosus (Fisher and Dunay, 1984)

Appendix A: Plate 4, specimen 4

Alete bisaccate pollen; outline diploxylinoid. Corpus oval to circular in outline, longitudinal axis slightly greater than transverse axis. Corpus exine punctuate, approximately 2 µm thick. Cappa and cappula not strongly differentiated although there is evidence of exinal thinning on the distal surface. Sacci small, approximately 1/3 corpus size, and globular. Proximal attachment barely supra-equatorial, distal attachment sub-equatorial: sacci distally inclined. Sacci finely infrareticulate. No sulcus observed.

Equatorial diameter: 78-95 µm

Corpus: 54-71 µm

Protodiploxylinus fastidiosus (Jansonius, 1962)

Appendix A: Plate 4, specimen 3

Renamed from *Klausipollenites fastidiosus* by Dunay and Fisher (1979).

Central body rounded oval, bladder approximately circular, with straight distal bases. Sacci smaller than half the central body, intramarginal overlap almost 75%. Therefore in outline sacci joining the corpus at a very obtuse angle. Central body moderately thick, proximal side with infrareticulate exoexine. Sacci proximally attached subequatorially, distal displacement considerable. Distal bases only half the length of the chord at this position. Reticulation moderately fine (0.5-1 μm).

Breadth: 50-55 μm

Corpus: 40-45 μm

Dunay and Fisher (1979) argue that the genus *Microcachrydites* can be completely subdivided into species of *Protodiploxylinus*. Litwin (1986) determines two species of *Microcachrydites*, namely *Microcachrydites fastidiosus* (Litwin 1986: plate 14, palynomorph 4) and *Microcachrydites doubingeri* (Litwin, 1986: plate 14, palynomorph 3). The plate specimen of *Microcachrydites fastidiosus* is derived from the description of *Klausipollenites fastidiosus* (Jansonius, 1962) and has been reassigned to *Protodiploxylinus fastidiosus* (Dunay and Fisher, 1979). Dunay and Fisher (1979) argue for the reassignment of *Microcachrydites doubingeri* to *Protodiploxylinus doubingeri*. However, since no plate specimen is provided and the plate specimen provided by Litwin (1986) seems simply to be a junior type of *Protodiploxylinus fastidiosus*, these authors argue in favour of assigning *Microcachrydites doubingeri* and *Protodiploxylinus doubingeri* to *Protodiploxylinus fastidiosus*.

Rugubivesiculites proavitus (Fisher and Dunay, 1984)

Appendix A: Plate 6, specimen 3

Alete bisaccate pollen grain, outline diploxylinoid. Corpus oval, with longitudinal axis longer than transverse axis. Exine moderately thick (ca. 2-2.5 μm), punctate; proximally ornamented with rugulae up to 24 μm long and 4 μm wide. Distally with an unornamented oval leptoma. Sacci large, kidney shaped and distally pendent. Saccus infrastructure indistinct, probably finely and irregularly infrareticulate although radially oriented compression folds are clearly visible.

Equatorial diameter: 115-76 μm

Corpus: 65-44 μm

Samaropollenites speciosus (Dolby and Balme, 1976)

Appendix A: Plate 5, specimen 4

Pollen disaccate or bilaterally symmetrical monosaccate, haploxylinoid or slightly diploxylinoid. Corpus transversely elongate oval, proximal surface pronouncedly convex, distal surface flattened. Cappa 2-4 μm thick, finely and densely columellate appearing evenly punctate in surface view. Sacci strongly distally inclined, joined sub-equatorially in most specimens by narrow bands of slightly inflated exoexine to enclose an oval cappula. Sacci hemispherical in polar view, intrareticulate, with radially elongate brochi adjacent to the proximal bases. Cappula 1-3 μm thick, unstructured or faintly intragranulate. Breadth of cappula about one-third that of corpus.

Breadth: 56-87 μm

Corpus: 51-56 μm

Voltziaceasporites heteromorpha (Klaus, 1964)

Appendix A: Plate 6, specimen 5

Bisaccate pollen grain with largely variable shape and size of the sacci. Grain doesn't have an Y-mark. The exine of the corpus is smooth to finely punctate, distally between the sacci usually oval. The sprouting area is usually unclearly marked, somewhat broadly oval. The inner exine lies in a partially thickened, exoexinal mantle; it heightens towards the sacci on

the longitudinal side. Sacci equatorially attached, somewhat distally inclined. Because the cappa can be considerably thick, is in certain side views a sort of crest visible. In polar view between the exoexinal structure sometimes a kind of longitudinal differentiation, also are one or several thinnings or foldings, usually not commonly, possible. The form of the sacci is sometimes somewhat oval shaped, sometimes haploxylonoid, sometimes strongly deflated. Sometimes the pollen grain, corpus and sacci together, looks like a butterfly (the *Platysaccus* kind). Reticulation of the sacci is usually imperfect.
Equatorial diameter: 70-150 μm

Trilete monosaccate pollen

Tulesporites terraerubrae (Dunay and Fisher, 1984)

Appendix A: Plate 2, specimen 5

Zonate palynomorph amb circular. Corpus circular; irregularly infrarugulate to infrareticulate. A faint trilete mark is present which extends normally to the corpus periphery and occasionally onto the zona. Zona finely regulate.

Overall breadth: 52-75 μm

Vallasporites ignacii (Scheuring, 1970)

Appendix A: Plate 2, specimen 6

Microspore with a somewhat oval contour. The corpus is covered by an exine, which is ornamented with high, dense and disordered faults and rugulae. The outer rim of the spore is about 5 μm and is created by a thickening of the exine. Another thickening of the exine on the proximal side of the spore is a trilete mark. It is often hard to distinguish, because it is also densely and disorderly regulated and faulted, just like the rest of the exine.

Width: ~40 μm

Other monosaccate pollen

Cordaitina minor (Pautsch, 1973)

Appendix A: Plate 2, specimen 3

Monosaccate, greyish-yellow pollen grains of medium size. Outline circular to slightly trilobate; shape disc-like. Body usually without secondary folds, yellow or light brown, sometimes with a fine reticulum near the bladder roots. Bladder outline smooth. Reticulum near the bladder roots often disposed radially. Bladder roots circular, covering one another.

Equatorial diameter: 37-57 μm

Daughertyspora chinleana (Dunay and Fisher, 1979)

Appendix A: Plate 7, specimen 2

Alete monosaccate palynomorph, corpus circular to sub-circular. Exine two layered, equatorially thickened; ectexine and endexine usually smooth, sometimes infrapunctate. Saccus attached sub-equatorially on the proximal surfaces, totally enveloping the distal surface. Saccus circular to sub-circular, infra-rugulate; in the proximity of the corpus, the individual sculptural elements are radially oriented.

Overall breadth: 35-50 μm

Heliosaccus dimorphus (Fisher and Dunay, 1984)

Appendix A: Plate 2, specimen 8

Subcircular to subtriangular cavate palynomorph. Corpus subcircular to subtriangular; exine two-layered: endexine smooth, extexine finely and irregularly plicate or regulate. Trilete mark

small, simple and typically indistinct. Well defined circumpolar folds commonly present. Saccus irregular in outline; infrastructure indistinct with irregularly thickened radially arranged fimbriate elements adjacent to corpus but lacking all visible structure close to the periphery. Saccus of overall diaphanous appearance.

Description by Fisher and Dunay (1984) describing *Pachysaccus feroccidentalis*, but Litwin (1986) assigns *P. feroccidentalis* to *Heliosaccus dimorphus*.

Patinasporites densus (Scheuring, 1970)

Appendix A: Plate 2, specimen 1

Monosaccate pollen grain in proximal view. The pollen grain is circular, with a bulged central corpus exine. The distal side is a exine-free aperture, which has been interpreted as the oval sprouting area. This sprouting area is clearly visible. The monosaccus is in proximal view just a weak folding. Distally the monosaccus is partially underneath the corpus, because the corpus is about half the size of the total pollen grain. The contact are between the monosaccus and the pollen corpus can look like a bulgy thickening. The whole exospore is regulated with wavy and twisted ornamentation. The ornamentation is clearly more dense and more fine on the monosaccus.

Width: 40-70 μm

Monosulcate pollen

Cycadopites follicularis (Balme, 1970)

Appendix A: Plate 2, specimen 9

Monosulcate, amb oval, uncompressed specimens fusiform. Sulcus extending full length of grain often, not always, slightly narrower near the distal pole, margins of sulcus overlapping in some specimens. Exine about 1 μm thick, unsculptured, unstructured or faintly intragranulate.

Length: 35-54 μm

Breadth: 16-34 μm

Preticolpipollenites bharadwajii (Balme, 1970)

Appendix A: Plate 7, specimen 3

Amb oval, trisulcate. Median sulcus clearly defined and running the full length of the grain, extremities usually slightly expanded, and margins sometimes overlapping in the vicinity of the distal pole. Two slit-like lateral sulci arranged on either side of the prominent median sulcus and often accompanied by longitudinal folds. Extremities of lateral sulci somewhat convergent, but never joining to form a continuous "ring-furrow". Exine about 1 μm thick, faintly intrapunctate.

Length: 25-31 μm

Breadth: 17-24 μm

Spores

Equisetosporites chinleana (Daugherty, 1941)

Appendix A: Plate 2, specimen 4

A spherical spore with two tightly wrapped elaters which cannot be distinguished from of spores of modern members of the genus *Equisetum*. The spore wall is thin and is 36 microns in diameter.

Froelichsporites traversei (Litwin et al., 1993)

Appendix A: Plate 1, specimen 4

Azonate, tetrahedral obligate spore tetrads, rarely obligate tetrads with slightly to moderately thickened and fused curvaturae perfectae. Proximal face of each component spore in complete contact with all others. Ulcus present on exospores of each distal pole. Distal portion of spores commonly hemispherical. Spores double-layered; perispore and exospores each less than 1 µm thick. Tetrad occasionally exhibits only exospores on distal hemisphere of each of its spores, with remnant perispore adhering along and across the line of contact between spores.

Diameter: 45-73 µm

Dunay and Fisher (1979) assign the tetrahedral tetrad from Triassic sediments of the United States to *Pyramidosporites*. This genus is used until Litwin et al. (1993) assign it to the new genus *Froelichsporites*, arguing that the type species of the genus *Pyramidosporites* has some very distinct features from the material from the United States (Litwin et al., 1993 and references therein), and thus the American material needs a new genus.

Palaeobotanical affinities

Importance and methods assigning palaeobotanical affinities

In reconstructing the palaeo-environment from a palynofloral assemblage, it is important to be able to assign typical palynomorphs to a type of botanical taxon. However, the only method of assigning palynomorphs to a macrofossil taxon, is to find the palynomorph in direct association with or even *in situ* with the male cone or sporangium. It is therefore not surprising that most pollen and spore taxa from the dispersed record do not have a macrofossil associated with them. This is most likely due to the fact that pollen can be transported over long distances and, especially in the case of the palaeo-environment of the late Triassic in southwest USA, the macrofossils from upland vegetation types are unlikely to be preserved (Demko et al., 1998; Ash, 1999). Moreover, the preservation potential of pollen and spores is higher than macrofossils. Even when pollen and spores can be found in direct association with its pollen or spores, it can be the case that the plant produces several kinds of pollen or spores, or that several plants produce the same type of pollen or spores. Therefore, it is often difficult to assign pollen and spore species to specific plant species or even genera. Some pollen and spore types are distinct enough to be able to assign them to specific families, but one has to settle with assigning them to a certain division or even lower ranks of classification.

By far the most common pollen types in the sediments of the Chinle Formation are those produced by Gymnosperms, likely to be mostly conifers. In the macrofossil record, most Paleozoic conifer families have gone extinct at the end of the Permian, save the Voltziaceae, which survive into the Jurassic (Farjon, 2008). It is however likely that a number of Paleozoic conifer families simply remain unpreserved as they only occur as upland vegetation (Van Konijnenburg-Van Cittert, pers. comm.). Mesozoic conifer families may also have occurred earlier than is known from the macrofossil record. In the late Triassic, macrofossils of the Mesozoic conifer families Araucariaceae and Cheirolepidiaceae for example have been found (e.g. Alvin, 1982; Ash, 1999; Farjon, 2008). However, judging from the palynological record, it seems likely that for example the Podocarpaceae are also present in the late Triassic of North America.

In this study plant groups were derived from the botanical affinities of the palynomorphs and these were used to reconstruct the palaeo-environment (table 1) (Balme, 1995; Bonis, 2010).

Included is a short discussion for the affinities of several important palynomorphs of which descriptions can be found in the chapter on systematic palynology.

Pollen/spore species	Botanical affinity
Voltziaceasporites heteromorpha Voltziaceasporites globosus Triadispora dockumensis Triadispora fallax Platysaccus triassicus	Pinophyta (Voltziaceae)
Araucariacites sp. Patinasporites densus Daughertyspora chinleana	Pinophyta (Araucariaceae)
Camerosporites sp.	Pinophyta (Cheirolepidiaceae)
Angustisaccus reniformis Angustisaccus petulans	Pinophyta (Podocarpaceae)
Vallasporites ignacii Cordaitina minor Enzonalasporites vigens Pseudoenzonalasporites summus Klausipollenites gouldii Klausipollenites schaubergeri Klausipollenites lithodendrorum Klausipollenites vestitus Minutosaccus crenulatus Rugubivesiculites proavitus Samaropollenites concinnus Samaropollenites speciosus	Pinophytes of uncertain families Cordaitaceae (?)
Cycadopites fragilis Cycadopites follicularis Preticolpipoollenites bharadwajii	Other Gymnosperms (Cycadophytes)
Alisporites opii Chordasporites chinleanus Colpectopollis ellipsoideus Falcisporites nuthalensis Falcisporites gottesfeldi Protohaploxyypinus arizonicus Infernopollenites claustratus Vitreosporites pallidus Pityosporites devolens Pityosporites scaurus Pityosporites oldhamensis Protodiploxyypinus fastidiosus Protodiploxyypinus lacertosus Protodiploxyypinus ujhelyi Protodiploxyypinus americanus Protodiploxyypinus triquetricorpus	Other Gymnosperms (Ginkgophytes, Caytoniales, Glossopteridales, Bennetitales) Glossopteridales Caytoniales Bennetitales (?)
Equisetosporites chinleana	Other Gymnosperms (Gnetophyta)
Heliosaccus dimorphus Kuglerina meieri Ovalipollis ovalis Pseudoillinites crassus Pseudoillinites platysaccus Sulcatisporites krauselii Schizosaccus keuperi Guthoerlisporites cancellous Lagenella martini Plicatisaccus badius	Gymnosperms of uncertain affinities
Convolutispora klukiforma Dictyophyllidites harrisii Kyrtonisporis speciosus Staplinisporites telatus Osmundacidites wellmannii Todisporites major Verrucosisporites tumulosus	Pteridophyta Dipteridaceae/Matoniaceae Osmundaceae Osmundaceae Osmundaceae
Calamospora tener	Sphenopsida
Retriletes gracilis	Lycophyta
Stereisporites nochtensis	Bryophyta
Foveolatisporites potniei Nevesisporites sp. Krauseliiisporites cooksonae Froelichsporites traversei	Spores of uncertain affinities

Table 1: Botanical affinities of important pollen and spores of the Chinle Formation used and discussed in this study.

Coniferous pollen types

The Voltziaceae represent the last family of Paleozoic conifers in the Mesozoic (Farjon, 2008), at least assuming the macrofossil record as representative and that none of the other Paleozoic conifer families survived the Permian-Triassic crisis. The genera *Voltziaceasporites* and *Triadispora* are associated with this family (Balme, 1995 and references therein).

Three Mesozoic conifer families are represented in the palynological record of the Chinle Formation; the Araucariaceae, the Cheirolepidiaceae and the Podocarpaceae.

Examples of *Araucariacites* are found in the record and the presence of Araucariaceae seems logical given the large amount of fossilized stems of *Araucarioxylon arizonicus* (e.g. Ash and Creber, 1992). The large amount of stems this species suggests a dominance of Araucariaceae type conifers as upland species, whereas the amount of *Araucariacites* type pollen in the palynological record is not commonly present. The genus *Patinasporites* has been suggested as having affinity to the family Cheirolepidiaceae (Cornet, 1977). However given the morphological features of *Patinasporites* and the abundance of *Araucarioxylon arizonicus* as a macrofossil, it seems likely that *Patinasporites* has affinities with the family Araucariaceae as well (Van Konijnenburg-Van Cittert, pers. comm.). The same goes for the discussed genus *Daughertyspora*, which has been recognized as a separate genus from *Patinasporites* (Dunay and Fisher, 1979), but shares significant characteristics with *Patinasporites*. It is hereby suggested that if *Daughertyspora* is a separate genus, it has a close relationship to *Patinasporites* and is therefore also most likely part of the family Araucariaceae.

The genus *Camerosporites*, a member of the circumpolloid group, is held in association with the conifer family Cheirolepidiaceae (Zavialova and Roghi, 2005). *Camerosporites* is most likely the only representative of the Cheirolepidiaceae in the Carnian and Norian of the Chinle Formation.

The third Mesozoic conifer family is the Podocarpaceae. The genus *Podosporites* was recognized in the continental deposits of the Carnian and Norian of the Dockum group (Dunay and Fisher, 1979), but was later determined to be the different but closely related genus *Angustisaccus* (Fisher and Dunay, 1984). This is most likely the only representative of the Podocarpaceae and is probably only found in upland flora, because macrofossil representatives of the Podocarpaceae have never been described from North America.

There are several other genera, probably representants of conifer families, of which the exact affinity is uncertain (table 1), *Vallasporites* and *Enzonalsporites* are important examples. They are often found in association with *Patinasporites* and *Daughertyspora*.

Another important genus is *Cordaitina*. It has been found in situ in sediments of the Carboniferous with representatives from the Cordaitales and in the Permian with representatives from the Emporiaceae (Balme, 1995 and references therein). There is no record of macrofossils of the Emporiaceae and Cordaitales following the Permian mass extinction (e.g. Farjon, 2008). It is likely that representatives of the Cordaitales survived in refugee areas longer than is shown in the macrofossil record (Kirkland and Frederiksen, 1970), therefore the very distinct *Cordaitina* pollen found in the Chinle Formation are in this study associated with descendants of the Cordaitales. The relatively common macrofossil genus *Pelourdea* from the Chinle Formation has been associated with the Cordaitales (Ash, 1987). However, male cones were never preserved and it is therefore not confirmed that *Pelourdea* is actually a member or a descendant of the Cordaitales or is actually unrelated.

A very important pollen genus is *Klausipollenites*, because it is dominant throughout most of the investigated sections. The affinity of this genus is unknown. It most likely represents a type of conifer. These authors have assigned *K. gouldii* to the Mesozoic conifer group judging from its morphological features and its distribution.

Other Gymnospermous pollen types

Two microfossil representatives of the Cycadales are found in the sediments of the Chinle Formation. *Cycadopites* has been found *in situ* in many Cycadalean and Bennettitalean macrofossils. *Cycadopites* has remained virtually the same since the first occurrence of the genus. *Preticolpipollenites* varies only slightly from *Cycadopites* and also represents a member of the Cycadales (Balme, 1970).

Most other Gymnosperm types tend to get lumped together, due to the uncertainty in distinguishing specific characteristics, or the relevance of the plant type to the study. A clear example is the bisaccate genus *Alisporites*. The tendency in Mesozoic and Palaeozoic palynology is to lump morphologically very dissimilar bisaccate pollen types together as *Alisporites*. *Alisporites* has therefore been found in association with several types of conifers, Ginkgoales and seed ferns (Balme, 1995 and references therein). In this study only one species of *Alisporites* has been used: *Alisporites opii*. This genus can be narrowed down more precisely for its morphological features. It is most likely not dispersed by a type of conifer. It does not have features commonly associated with Glossopterids. These authors assign it to Ginkgoales, Bennettitales or Caytoniales, which is still a rather broad distinction.

Bisaccate pollen genera with striations or intra-exinal thickenings are often associated with Glossopterids. The most common example from the Chinle Formation is the genus *Chordasporites*, however this genus has never been found *in situ*. *Protohaploxylinus* is less common in the Chinle Formation, but has been found *in situ* in Permian sediments with Glossopterids (Balme, 1995 and references therein).

Several important bisaccate pollen have been a topic of discussion. *Protodiploxylinus* and *Pityosporites* are common as dispersed bisaccate pollen in the Chinle Formation and strongly resemble conifer pollen types of either Pinaceae or Podocarpaceae. These pollen types have been found *in situ* with the male organ *Pramelreuthia* which is most likely a Bennettitalean cone (Ash and Litwin, 1996) and certainly not a conifer cone.

There are still several kinds of pollen which have not been found *in situ* and can not be distinguished to a certain group of Gymnosperms on bases of their morphology (table 1).

Spore producing plant types

Spores are rare in comparison to pollen in the Chinle Formation. In comparison to pollen producing plants, spore-producing plants are far less productive, especially when considering that insect pollination was less important in the late Triassic than it is now. The sphenopsids, which represent an important group of riparian vegetation throughout the Chinle Formation and can be found abundantly as macrofossils (e.g. Ash, 1980), are underrepresented in the microfossil record. The only genus representing the sphenopsids is *Calamospora*.

There are very few genera in the Chinle Formation representing lycopsids and bryophytes. Pteridophytes have a larger representation in the Chinle Formation of which *Osmundacidites*, *Todisporites* and *Dictyophyllidites* are the most important. Each of these genera has been found *in situ*; *Osmundacidites* and *Todisporites* in ferns belonging to the Osmundaceae and *Dictyophyllidites* to the Dipteridaceae and/or Matoniaceae (Balme, 1995 and references therein). Lastly, *Froelichsporites* represents an important component of the sporomorph assemblage of the Chinle Formation, especially in higher sections. However, this genus has not been found *in situ* and it does not have distinct morphological features that can assign it to a specific plant group apart from the usual spore producing plants. The species typical for the Chinle Formation, *Froelichsporites traversei*, is described as a tetrahedral tetrad with a smooth exine and raised commisures (Dunay and Fisher, 1979). The occurrence of tetrahedral tetrads has been associated with herbaceous lycopsids occurring after the Permian-Triassic mass extinction (Visscher et al., 2004). The resemblance of *Froelichsporites*

traversei to the tetrahedral tetrad of *Densoisporites* might indicate that *Froelichsporites traversei* is dispersed by lycopsids. However, it is important to note that there is no known single occurrence of *Froelichsporites traversei*.

Results

Palynoflora

The Devil's Playground section yielded broad diverse palynofloral assemblages. Among the clearly dominant gymnospermous pollen, a clear overrepresentation of a sole pollen type is absent. The pollen taxa characterizing the assemblage at this section are *Samaropollenites speciosus*, *Samaropollenites concinnus*, *Kuglerina meieri*, *Cordaitina minor*, *Vallasporites ignacii*, *Angustisaccus reniformis*, *Triadispora fallax*, *Minutosaccus crenulatus* and several species of the genus *Protodiploxypinus*. Spore taxa are rather rare, in places taking up as little as 2 percent of the assemblage (fig 5).

The next part of the investigated interval includes a hiatus of ~2.3 meters. Sections spanning this interval were the upper part of the Mountain Lion Cliff section and the Silcrete Butte's section (fig 4), however neither of these sections proved to be productive. Given the broad exposure at Petrified Forest National Park, it seems likely the interval should be exposed elsewhere and might prove productive.

The following part of the investigated interval is exposed at the Badlands section. Between 96.5 and 97 meters (fig 5) there is a short-lived interval where spore taxa are abundant in comparison to the lower part of the section as well as the Devil's Playground section. These spore taxa include *Dictyophyllidites harrisii*, *Osmundacidites wellmannii* and *Todisporites major*. Some pollen taxa, *Araucariacites sp.* and *Preticolpipoollenites bharadwajii*, together with the spore taxa become more abundant in this relatively short interval. The pollen taxa which are important in the Devil's Playground section become less abundant and others disappear altogether. *Klausipollenites gouldii* in particular shows a very significant change at this interval as it becomes by far the most dominant pollen type, at some intervals comprising over 50% of the assemblage.

Above 97 meter the spore taxa become a minor part of the assemblage again. *Klausipollenites gouldii* is still by far the most abundant pollen type, but other pollen taxa reappear in low abundances. Such taxa include *Schizosaccus keuperi*, *Enzonalasporites vigenis*, *Chordasporites chinleanus* and *Triadispora dockumensis*. One taxon makes its first appearance in this section, *Froelichsporites traversei* (fig 5). In this part of the section the pollen taxon *Patinasporites densus* becomes more abundant as well.

The abundant *Klausipollenites gouldii* also boasts rather distinct morphotypes. These different morphotypes will be discussed further in the section 'Discussion'. The diversity of morphotypes of *K. gouldii* increases after the hiatus in the palynological record.

The general trend in the palynofloral composition of this part of the Sonsela Member is a decrease in diversity, whereas the pollen taxon *Klausipollenites gouldii* becomes the most abundant palynomorph. There is a short interval where several spore taxa are fairly abundant in comparison to other parts of the section. Full species abundances throughout the sampled interval provided in Appendix B. A complete qualitative analysis can be found in appendix C.

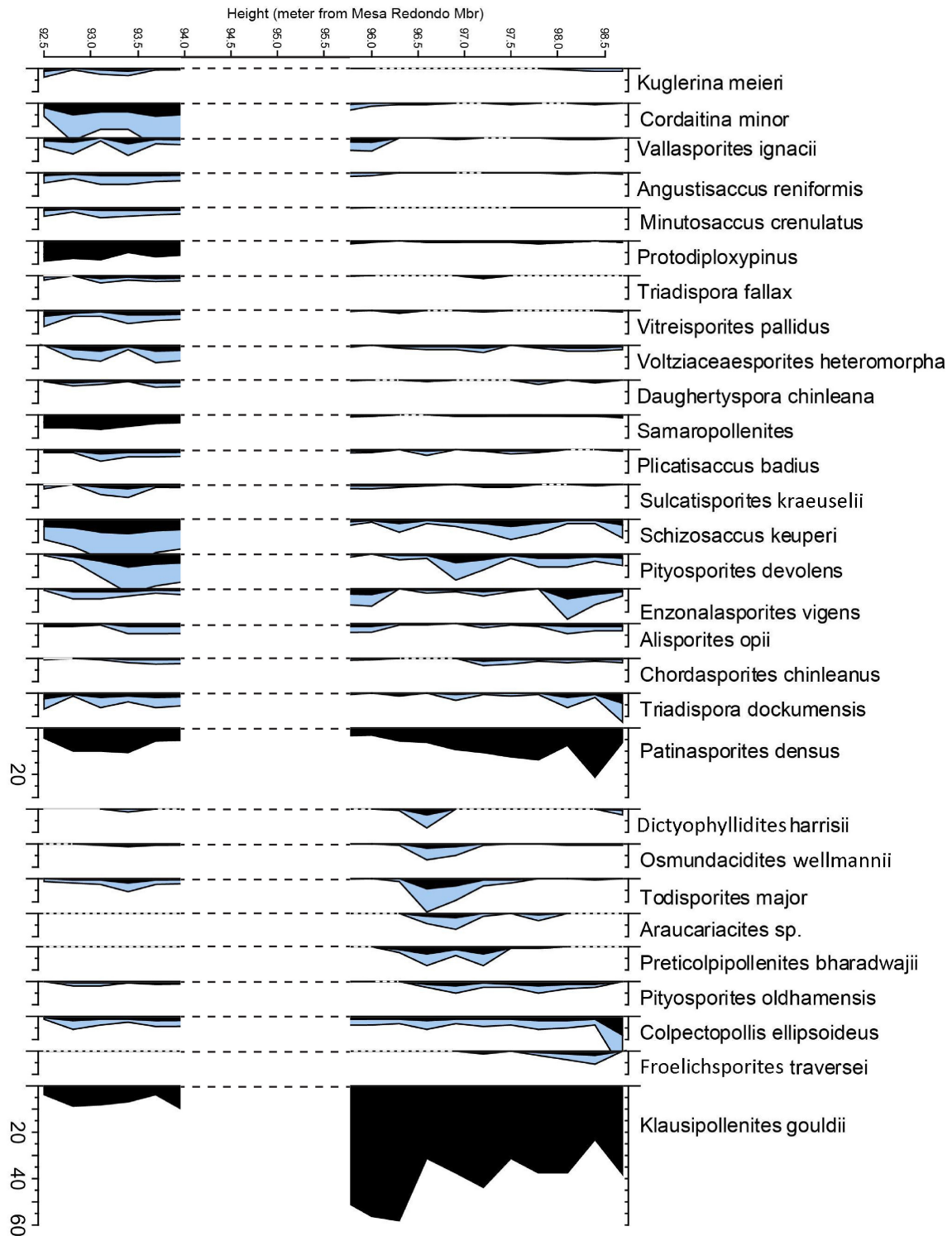


Figure 5: Relative species abundances, plotted along height from Mesa Redondo Mbr. Black outline: actual species relative abundances, blue outline: exaggeration (x3).

Cuticula

The Devil's Playground section in the lower part of the Jim Camp Wash beds contained an overall diverse flora. An important component of these strata were the ginkgophyte genus *Baiera* and the cycadophyte *Nilssonia* (Ash, 2001). The coniferous leaf genera *Pagiophyllum* (Ash, 1970b, 1978) and *Brachyphyllum* (Ash, 1973) also occurred, though less abundantly.

The Badlands section yielded a flora where *Baiera* and *Nilssonia* were not present. The most important components of this section are several as yet unidentified species of cycads or cycadeoids. There are still occurrences of *Pagiophyllum* and *Brachyphyllum*, though less abundant and *Dinophyton* is found in this section. It is likely though that *Dinophyton* (Ash, 1970a) also occurred in the Devil's Playground section, but it did not lacerate well and was therefore unrecognizable.

$\delta^{13}\text{C}_{\text{TOC}}$ and total organic carbon percentage

The $\delta^{13}\text{C}_{\text{TOC}}$ record shows strong variation throughout the sampled interval. The lower part of the Mountain Lion Cliff section including the sample from within the Jasper Forest bed show a rise from $\sim -27\text{‰}$ to $\sim -24\text{‰}$. The total organic carbon percentage stays roughly the same throughout the Mountain Lion section, never exceeding 1.5%. Towards the top of the section the $\delta^{13}\text{C}_{\text{TOC}}$ value increases. There is a large spike in the total organic carbon percentage in the lower part of the Devil's Playground section, this spike corresponds with a relatively low $\delta^{13}\text{C}_{\text{TOC}}$ of -24‰ and throughout the Devil's Playground section the $\delta^{13}\text{C}_{\text{TOC}}$ values linger around this value, although total organic carbon percentages aren't as high. Within the Badlands section total organic carbon percentages linger around the 1% and $\delta^{13}\text{C}_{\text{TOC}}$ values drop to -29‰ . Within the Mountain Lion Mesa section the total organic carbon percentages stay low and the $\delta^{13}\text{C}_{\text{TOC}}$ values stay relatively high around $-24,5\text{‰}$, but rising to about $27,5\text{‰}$ towards the top of the section (fig 6).

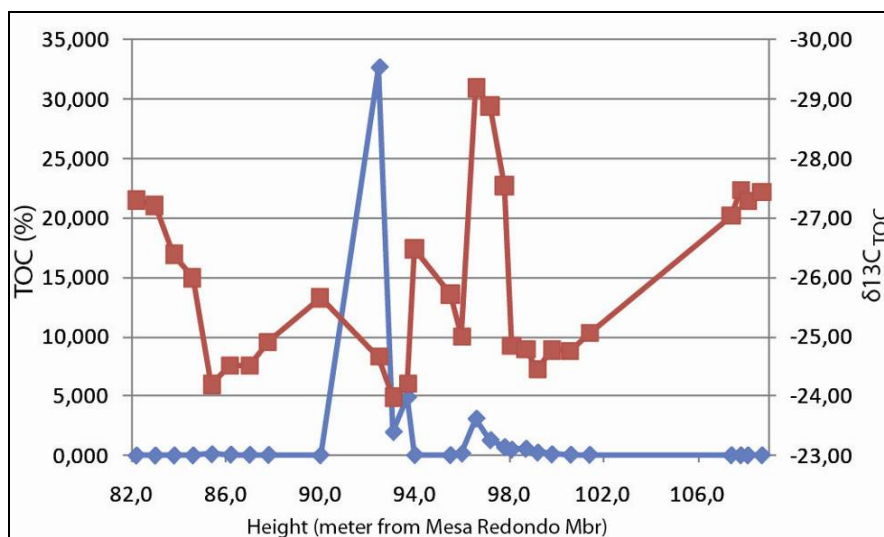


Figure 6: $\delta^{13}\text{C}_{\text{TOC}}$ (red line) and total organic carbon percentage (blue line) plotted against height in meters from the Mesa Redondo Member.

PCA

Principal Components Analysis was performed on the palynomorph and environmental proxy data on the productive samples from Petrified Forest National Park. The PCA plot shows that 28% of the variation can be explained with the variation on the x-axis whereas 12% of the variation can be explained with the variation on the y-axis. *Klausipollenites gouldii* corresponds strongly inversely with the x-axis, whereas a number of taxa, *Protodiploxypinus lacertosus*, *Cordaitina minor*, *Angustisaccus reniformis*, etc., respond in exactly the opposite way (fig 7). Several pollen taxa and most spore taxa seem to correspond more closely to variations on the y-axis, in particular *Todisporites major* and *Osmundacidites wellmannii*. Other taxa respond inversely to the y-axis, such as *Froelichsporites traversei* and *Chordasporites chinleanus*, however these taxa do not respond as strongly as the taxa on the positive side of the y-axis do. This plot shows only a selection of the pollen and spore taxa to. Several taxa with low abundances were omitted from the PCA plot, as well as taxa which showed weak correspondence to any of the axes.

Other parameters measured were also included in the PCA analysis; the abundance of xenomorphs and the $\delta^{13}\text{C}_{\text{TOC}}$ values (fig 7). These two parameters seem to be inversely correlated to each other, which would mean that the when $\delta^{13}\text{C}_{\text{TOC}}$ values decrease, the amount of xenomorphs increase.

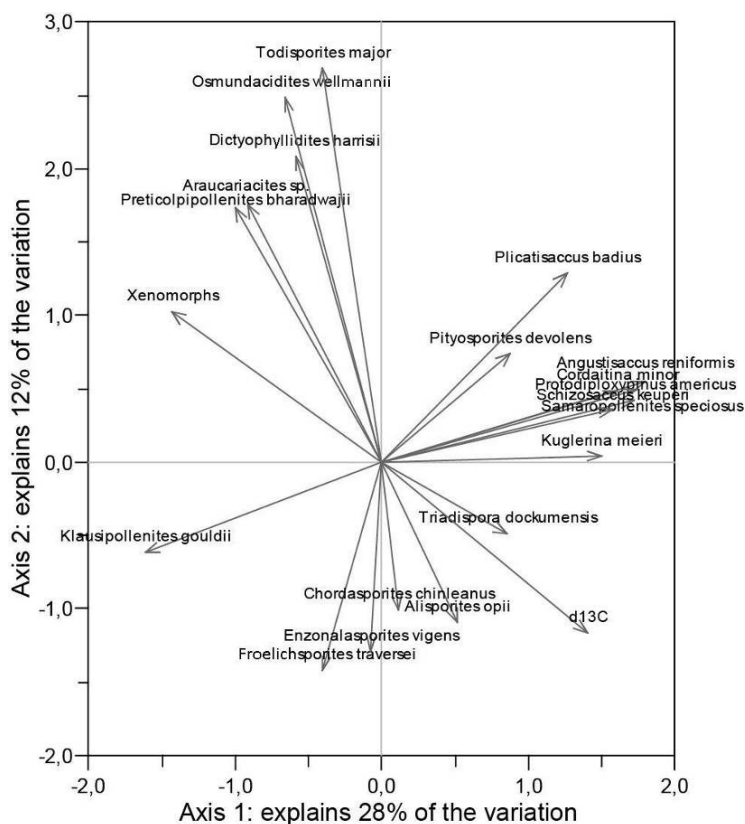


Figure 7: Plot of the Principal Components Analysis performed on the palynomorph and environmental proxy data from the productive samples at Petrified Forest National Park. Note that the larger part of the species have been omitted from the plot.

Discussion

Palaeo-environment

Since the eighties, interpretation of the facies within the Chinle Formation have shown large differences. The presence of coal beds together with a seemingly tropical flora (e.g. Ash, 1980) is in strong contrast with the interpretation of the sedimentary facies, which suggest an arid to semi-arid environment with strong seasonality (Dubiel et al., 1991). It is most likely that the depositional environment of the Chinle Formation was not tropical, but that the localized coal deposits represent riparian vegetation in lowland environments (Demko et al., 1998), whereas the dominant upland vegetation was semi-arid (Ash, 1999). From the study of paleosols it has been confirmed that the overall depositional environment of the Chinle Formation had low annual precipitation rates (Prochnow et al., 2006) and the general trend

towards the end Triassic was aridification (Cleveland et al., 2008). Two important driving forces were responsible for aridification of the depositional environment of the Chinle Formation. Over the late Triassic the amount of atmospheric CO₂ increased due to the rifting apart of Pangaea, causing globally increased temperatures and shifting of climatic zones (Tanner et al., 2004). The North American continent was moving in a northward direction, causing the depositional environment of the Chinle Formation to move from tropical latitudes towards mid-latitudes (Cleveland et al., 2008). This also attributed to the overall aridification in the late Triassic.

From the palynological record it becomes evident that the regional vegetation type was

dominated by Mesozoic conifers (Araucariaceae, Podocarpaceae, Cheirolepidiaceae) and Pteridosperms (fig 8), assuming that the very dominant pollen type *Klausipollenites gouldii* is produced by an upland Mesozoic conifer. The large offset between the macrofloral record and the dispersed palynological record supports the idea of a semi-arid environment where drought tolerant upland vegetation comprises the largest fraction of land cover, but is very unlikely to be preserved due to the lack of water bodies (Ash, 1999; Demko et al., 1998).

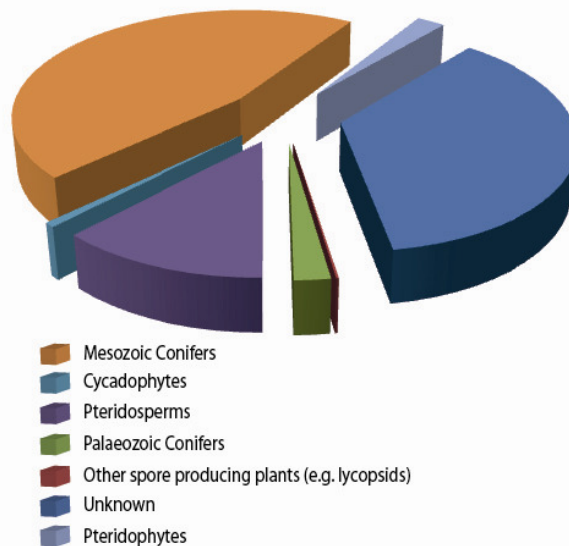


Figure 8: Pie chart of overall plant type percentages, derived from the palynological record from the investigated interval.

Fauna change – flora change

Litwin et al., (1991) suggested a palynoflora zonal transition in the Sonsela Member within a stratigraphic interval which was determined by Martz & Parker (2010) to be analogous to the Jasper Forest bed and the Jim Camp Wash beds. Parker and Martz (in press.) established that a faunal turnover takes place within the Jim Camp Wash beds at a horizon of persistent red silcrete at Petrified Forest National Park. In this study the zonal transition between Litwin’s Zone II and Zone III has been narrowed down to an interval of about two meters within the Jim Camp Wash beds (fig 2 & 10). This interval also spans the silcrete horizon at which the faunal change of Parker and Martz (in press.) occurs. Therefore we can say that within the Sonsela Member (Norian) at Petrified Forest National Park a palynoflora change occurs within an interval of two meters of a faunal change. It is unlikely that the change in palynoflora found between the Devil’s Playground section and the upper sections (Badlands section and Mountain Lion Mesa section) can be explained by provincialism, due to the long range of pollen dispersal and the short distance the two sections are apart.

The overall dominance of pollen over spores can be attributed to the highly seasonal environment of the southwestern USA in the late Triassic (Demko et al., 1998; Prochnow et al., 2006), wherein the plants present had to be capable of surviving long periods of drought. Pteridophytes and Lycophytes probably mostly occurred in riparian lowlands (e.g. Ash, 1972, 1980), which were a minor part of the general environment. The upland environment was much more common, even though the preservation of an upland ecosystem is much more unlikely.

At the interval of palynoflora change several types of pollen disappear or drop significantly in abundance (e.g. *Cordaitina minor*, *Protodiploxypinus*). Pteridosperm pollen become much more uncommon, Palaeozoic conifer pollen become much less abundant and there is a large increase in Mesozoic conifer pollen (fig 9). However, this increase is attributed

to the increase of one type of conifer pollen: *Klausipollenites gouldii*, which these authors have assigned to Mesozoic conifers, but has never been found in situ. The possibility remains that this is actually an upland Pteridosperm. *Klausipollenites gouldii* is most probably dispersed by an opportunist, benefiting from the disappearance of the other taxa.

We can recognize an occurrence of a short increase in spore taxa (e.g. *Osmundacidites wellmannii*, *Todisporites major*). These spore taxa occur throughout the record, but at low abundance. Only just above the interval of fauna change do the spore abundances increase. These spore taxa are known to be tolerant of a wet environment and/or a higher water table (van Konijnenburg-van Cittert, pers comm.). The increase in spore taxa might indicate a short lived period with an increased humidity. The spore taxa appear at the same interval where the diversity suddenly drops. We can recognize some taxa which do not disappear at the interval of change, but become less abundant. After the interval of change these taxa increase in abundance again (e.g. *Enzonalasporites vigenis*, *Chordasporites chinleana*).

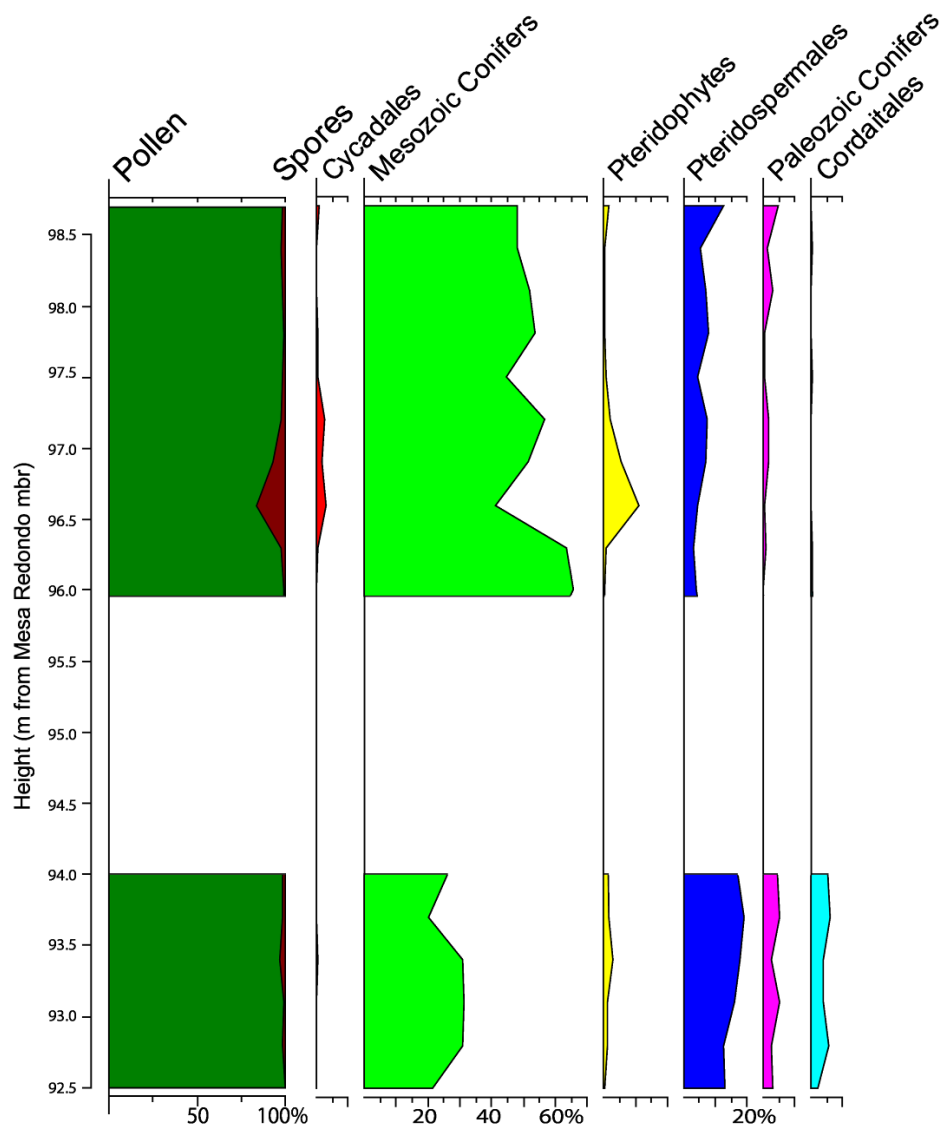


Figure 9: Percentages of plant types throughout the investigated interval.

The zones in this study were constructed on bases of changes in the palynofloral record (fig 10). They are not to be confused with the zones used in Litwin et al., (1991) pollen scheme. Zone 1 corresponds to a period preceding the interval of turnover; there is no clear dominance of a certain taxon and the record is relatively diverse. Zone 2 was based on the occurrence of taxa which are common in this zone, but nowhere else, such as the spore taxa. Zone 3 is the post-turnover zone; the spore taxa are decreasing in abundance and several types of pollen which were abundant in Zone 1 are increasing in abundance again.

The dissimilarity in the dispersed cuticula record recovered from the Devil's Playground section and the Badlands section can be interpreted as a change in flora as well. However, dispersed cuticula are very prone to be influenced by provincialism. Therefore the difference in the two records is not sufficient to say that a substantial change in macroflora occurred. Records need to be investigated from the same intervals to investigate the reality of this change.

Although the amount of time spanning the interval of change cannot be closely approximated, it is unlikely that a large hiatus in time is present at this interval, because no large erosional surfaces are known from this interval (Martz and Parker, 2010). The changes probably span a relatively short amount of time. Thus the turnover can't be attributed to slow forces of climate change such as slow northward drifting of the continent (Cleveland et al., 2008) or increasing atmospheric CO₂ concentrations due to the rifting apart of Pangaea (Prochnow et al., 2006; Tanner et al., 2004). An additional process must have been emphasizing the forces that changed the environment causing a prominent faunal and floral turnover. Whether this turnover occurred regionally or locally remains to be investigated. Most probably the change occurred regionally, for floral and faunal zones have been erected across continental deposits from North America and Europe, spanning this interval (e.g. Cornet, 1993; Heckert et al., 2007). However, locally continental deposits are difficult to correlate, regionally it is even more of a challenge (e.g. Cornet, 1993).

The occurrence of the tetrahedral tetrad *Froelichsporites traversei* provides a point of discussion. The abundance of this spore increases significantly after the proposed interval of turnover, if present at all before. The spore has been used as a marker for the Carnian (Litwin et al., 1991), but with recent revisions of the Carnian-Norian boundary (Furin et al., 2006) it becomes useless for this purpose. Litwin et al. (1991) find *F. traversei* in sections above and below the proposed interval of change. Therefore, we can assume that the first occurrence of *F. traversei* was not after the proposed interval of turnover. However, Litwin et al. (1991) do not mention abundances. The increase in abundance of *F. traversei* found in this study could be linked to environmental mutagenesis. Environmental mutagenesis occurs under the influence of atmospheric deterioration (Foster and Afonin, 2005) and has been associated with modern environmental stress factors as well as after mass extinctions (Visscher et al., 2004). However, natural occurrences of tetrahedral tetrads are not unknown. It is probable that *F. traversei* only occurs in tetrads, especially as no single specimens have been found in this study. However, this does not explain the large increase in abundance of *F. traversei* in the upper Sonsela Member.

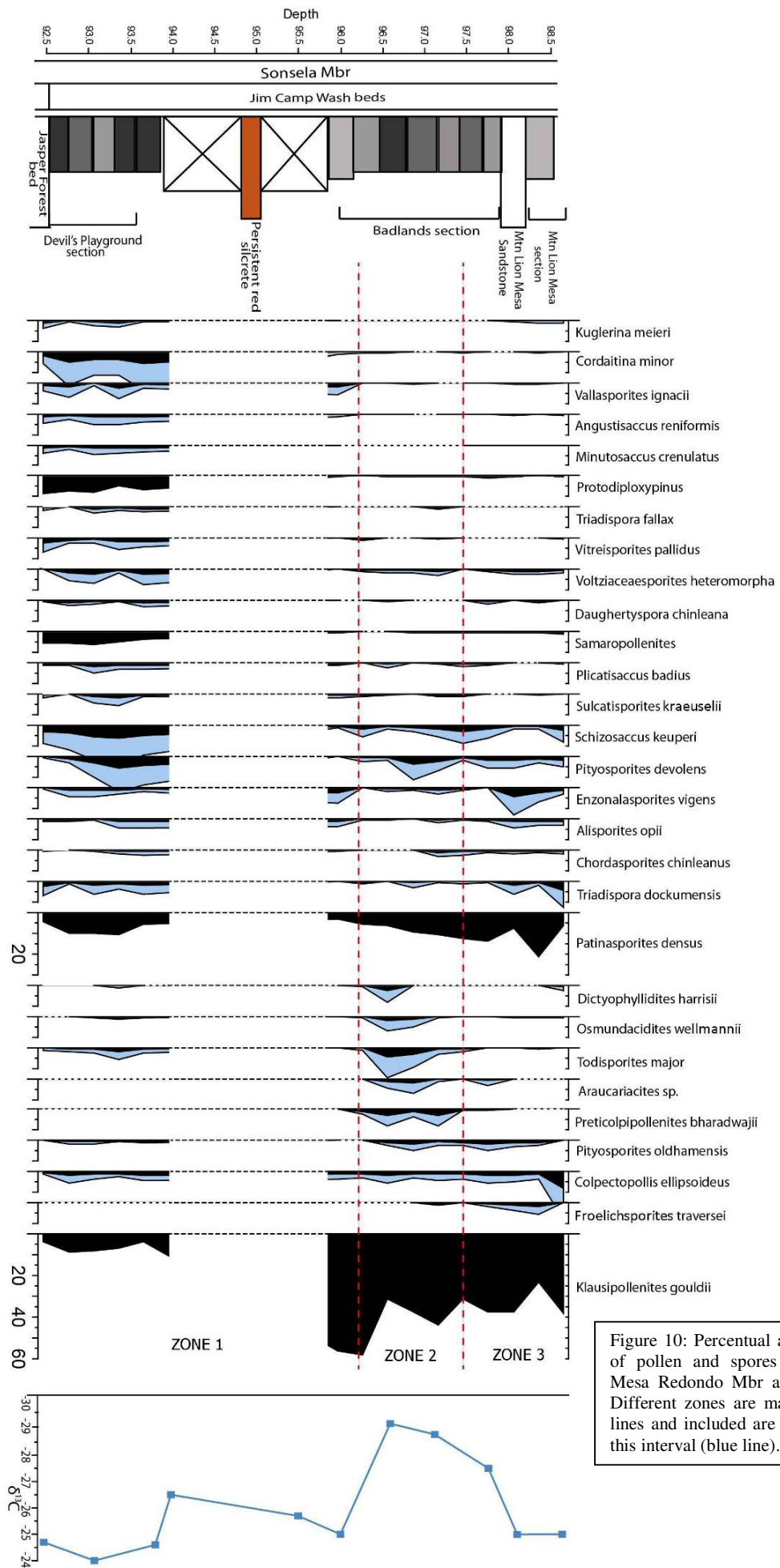


Figure 10: Percentual abundances of species of pollen and spores against height from Mesa Redondo Mbr and general lithology. Different zones are marked with red dotted lines and included are the $\delta^{13}C_{TOC}$ values of this interval (blue line).

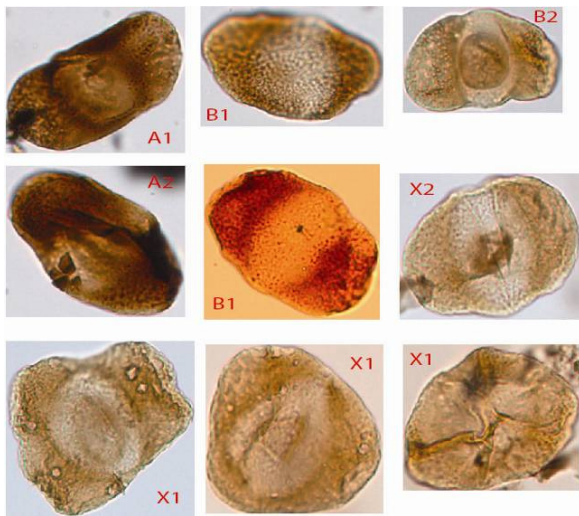


Figure 11: different morphotypes of *Klausipollenites gouldii*. Normal morphotypes A1, A2, B1 & B2 in the top two rows. Xenomorph X2 with a sulcus, middle row, far right. Different types of Xenomorph X1 in the bottom row. From left to right: Trisaccate, overgrown saccus and monosaccate.

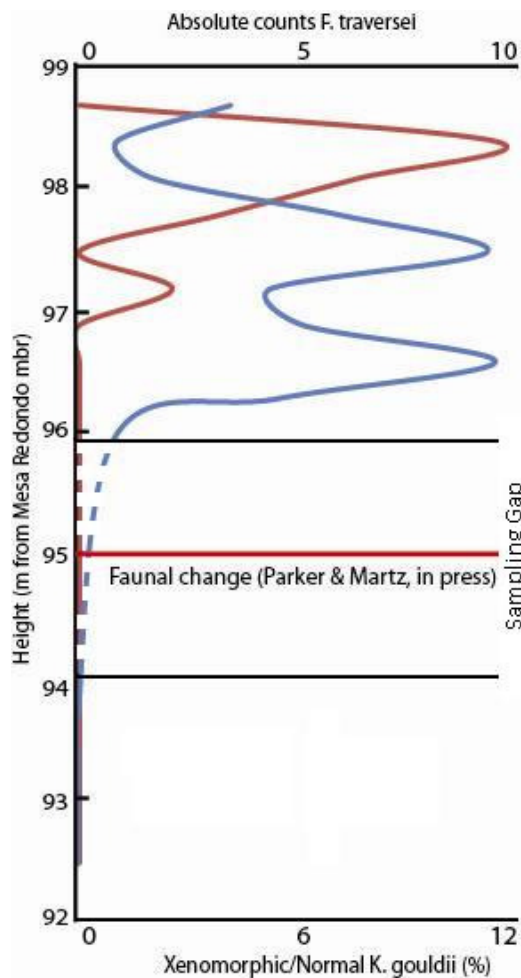


Figure 12: percentage of xenomorphic specimens of *K. gouldii* over normal specimens (blue line) and abundance of *F. traversei* (red line) versus height. The horizontal red line indicates where the proposed faunal of Parker and Martz (in press) occurs.

Another indication of environmental deterioration is the occurrence of xenomorphic subspecies (Foster and Afonin, 2005). The abundance and distinctness of *Klausipollenites gouldii* is good enough to determine several subspecies (fig 11) and to determine their changes throughout the investigated interval. Subspecies A1 and B1 are the most abundant and therefore probably represent the regular pollen types. The difference between the two is that A1 appears to be smoother whereas B1 is more poriferous. The subspecies A2 appears to have a longitudinal folding, which is suspected to be the result of compacting and is therefore not recognized in this study as a xenomorphic structure. Subspecies B2 has a circular dark spot in the middle of the corpus, which is most probably the germinal aperture of the grain. It is therefore not

recognized as a xenomorphic structure. Subspecies X1 has one 'overgrown' saccus or is trisaccate, sometimes close to monosaccate. These are not characteristics which can be attributed to the usual appearance of *K. gouldii* and has therefore to be interpreted as a xenomorphic structure. Subspecies X2 has a sulcus split, which is also a xenomorphic structure. Some specimens of *K. gouldii* are compacted which causes them to split down the middle and because of this a sulcus might be hard to determine. However, the material from Petrified Forest National Park was preserved well enough to determine if the pollen grains were influenced by compaction. Specimens of subspecies X2 were uninfluenced by compaction and still had the distinct sulcus. The increase of xenomorphic structures in *Klausipollenites gouldii* as well as the increase in abundance of *Froelichsporites traversei* both occur after the proposed faunal change by Parker and Martz (in press) (fig 12). If this increase can be attributed to a deterioration of the environment, it could have occurred at the same time as the change in fauna. However, due to the barren samples we discussed earlier, it is not yet possible to determine this with certainty.

The spike in *Froelichsporites traversei* occurs higher up in the section, but the general trend of both *F. traversei* and the xenomorphs of *Klausipollenites gouldii* is generally the same.

Possibly this is indicative of prevailing deteriorated atmospheric conditions. However, because we have no absolute time constraints on these sections, it is unknown how long these atmospheric conditions prevailed.

$\delta^{13}\text{C}_{\text{TOC}}$ and total organic carbon records

Both the $\delta^{13}\text{C}_{\text{TOC}}$ record and the total organic carbon record show a lot of variation. As there seems to be almost no correlation between the two (fig 13a,b,c) it can be assumed that another factor influences both parameters. The total organic carbon percentage in continental deposits is almost solely influenced by the depositional environment. As we have a range of total organic carbon from 0,01% to 32%, we can assume that the depositional environments of the samples were diverse. This could be the difference between a swamp and a settling pool of water cut off from the main stream of a river.

The difference in the $\delta^{13}\text{C}_{\text{TOC}}$ record is less clear. Ideally all the variance would be explained by changes in the $\delta^{13}\text{C}_{\text{TOC}}$ of the atmospheric CO_2 . However, here the variance between the different sections points to a different interpretation. Apart from the Badlands section, the $\delta^{13}\text{C}_{\text{TOC}}$ values stay above -27‰. For plant material, a stable carbon isotope value of below -27‰ is rather the rule than the exception (Boutton, 1991). Fresh water algae, which are most likely the most dominant components of the organic material of the Mountain Lion Cliff and Mountain Lion Mesa sections, have a much broader range of stable carbon isotopes in sediments (-35‰ to -15‰) than plant organic matter. The Devil's Playground section has stable carbon isotope values of around -24‰, about the same as the isotope values of the Mountain Lion Cliff and Mountain Lion Mesa sections, even though the Devil's Playground section is composed of similar sediments as the Badlands section.

The large differences between the various sections with different depositional environments is most likely caused by the difference in the source of organic matter. This would explain the large variances between the Mountain Lion Cliff and Mountain Lion Mesa sections and the Badlands section. However, it does not explain the difference between the Badlands section and the Devil's Playground section.

From the cuticular analysis it became evident that the floral composition of the Badlands section and the Devil's Playground section were thoroughly different. The different floral elements could fractionate carbon differently, which would explain the different $\delta^{13}\text{C}_{\text{TOC}}$ values. Another possibility is a change in the $\delta^{13}\text{C}_{\text{TOC}}$ values of the atmospheric carbon between the two sections. Key in this discussion is the $\delta^{13}\text{C}_{\text{TOC}}$ value of the lowest sample of the Badlands section, which is closer to the values of the Devil's Playground section (fig 14). This might be indicative of a change in $\delta^{13}\text{C}_{\text{TOC}}$ values within the Badlands section, which could mean a change in the composition of atmospheric CO_2 . However, the lowest sample of the Badlands section had a different composition; it had a lower organic carbon percentage and palynomorphs were poorly preserved. It might have been possible that the difference found between this sample and the other samples of the Badlands section is caused by a difference in the depositional environment.

When considering the data from the similar depositional environments, the difference between the Devil's Playground section and the Badlands section is significant. The differences within the Mountain Lion Cliff section and the Mountain Lion Mesa section can be attributed to varying input of organic detritus, however this is hard to investigate.

It is unlikely that the difference in $\delta^{13}\text{C}_{\text{TOC}}$ between the Devil's Playground section and the Badlands section is caused by the difference in vegetation, because vegetation generally has the same isotopic composition (Boutton, 1991). Alternatively the difference can be caused by an increased input of freshwater algae, however these have not been found in the palynological record.

Fig 13a: scatterplot of the Total Organic Carbon percentage of the samples from Petrified Forest National Park vs. the $\delta^{13}\text{C}_{\text{TOC}}$ of the same samples, including trendline.

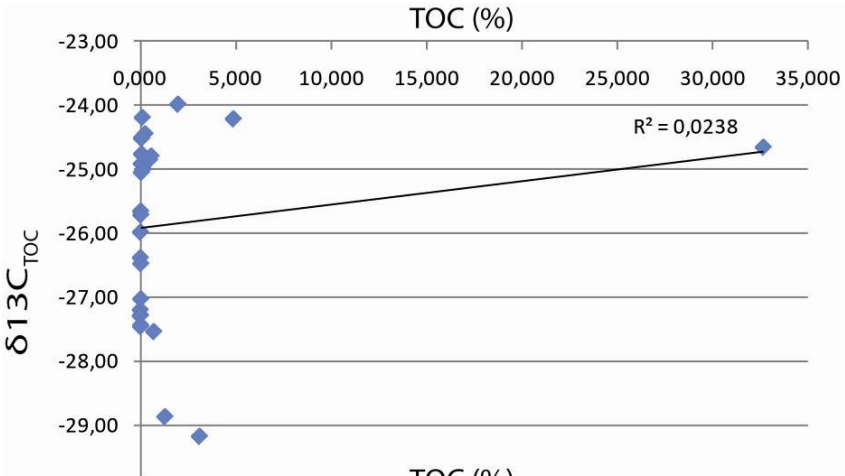


Fig 13b: scatterplot of the Total Organic Carbon percentage of the samples from Petrified Forest National Park with high organic carbon percentage (DP and BL sections, excluding BL1) vs. the $\delta^{13}\text{C}_{\text{TOC}}$ of the same samples, including trendline.

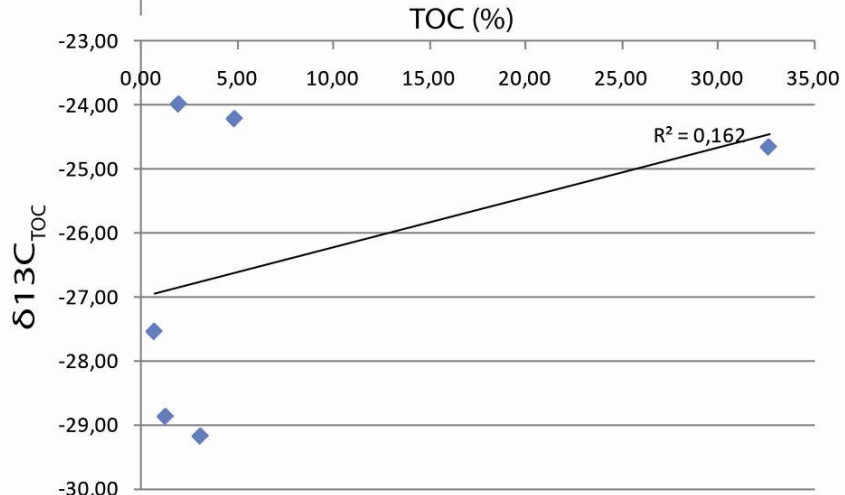
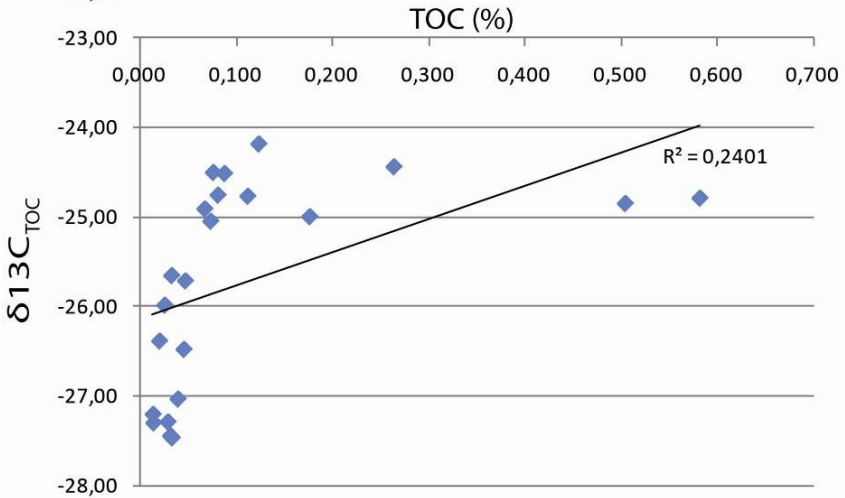


Fig 13c: scatterplot of the Total Organic Carbon percentage of the samples from Petrified Forest National Park with low organic carbon percentage (MLC, MLM sections + BL1) vs. the $\delta^{13}\text{C}_{\text{TOC}}$ of the same samples, including trendline.



The record of $\delta^{13}\text{C}_{\text{TOC}}$ in this section is not very detailed. Moreover there is a sampling gap if we only consider compositionally similar sediments. From this data it is therefore impossible to say whether the this change occurred gradually or rapidly. The changing isotopic composition could be attributed to variance in the water table as is also emphasized by the presence of humid tolerant sporomorphs in the upper section. The possibility remains that this change in $\delta^{13}\text{C}_{\text{TOC}}$ was caused by a change in the isotopic composition of atmospheric carbon, however there is no real evidence to support this theory. Ideally, $\delta^{13}\text{C}_{\text{TOC}}$

and paleosol isotopic composition would be determined at a high detail to investigate carbon cycle stability across the investigated interval.

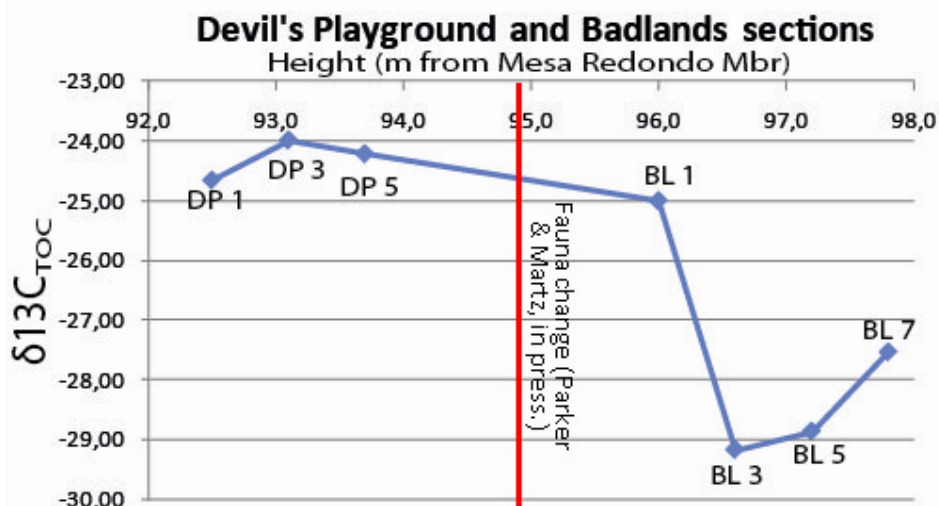


Figure 14: $\delta^{13}C_{TOC}$ vs. height of the Devil's Playground and Badlands section, showing sample numbers.

Principal Components Analysis

With the Principal Components Analysis (PCA) we can determine three distinct groups in the palynofloral record (fig 15). The group of taxa which respond negatively to the flora change, respond most strongly to the variance on the first axis, whereas the taxa dominant in Zone 2 respond the strongest to the variance on the second axis. *Klausipollenites gouldii* responds inversely to the group of taxa influenced negatively by the flora change. This becomes evident from the record (fig 10), because *K. gouldii* only becomes dominant where the other taxa disappear. Apparently *K. gouldii* responds positively to the environmental component which is making the other taxa disappear.

The amount of xenomorphs in *K. gouldii* and $\delta^{13}C_{TOC}$ values were plotted on the PCA to investigate how these parameters relate to the pollen and spore taxa. The amount of xenomorphs and the $\delta^{13}C_{TOC}$ values did not respond strongly to either axis and show no strong correspondence to the pollen and spore taxa. It is evident though, that both parameters respond inversely to each other. This suggests that when the amount of xenomorphic structures in *K. gouldii* increases, the $\delta^{13}C_{TOC}$ values drop. It has to be noted that in this PCA plot all values of the $\delta^{13}C_{TOC}$ were included and as we have seen from the data, this record is very sketchy. It is therefore not possible to say if these parameters actually do have an inverse correspondence to each other.

The abundances of xenomorphs and of *F. traversei* do not respond to the same factors, as becomes evident from the PCA-plot. Although both xenomorphs and the occurrence of tetrahedral tetrads can be associated with environmental deterioration (Visscher et al., 2004; Foster and Afonin, 2005), they apparently in this case do not occur simultaneously. It is also notable that *F. traversei* responds almost inversely to the spore taxa in Zone 2. This also becomes clear from the species data: *F. traversei* only becomes abundant after the spike in spore taxa (Zone 3), whereas *K. gouldii*, including the xenomorphs, has already become the most abundant component of the section during the spike in spore taxa (Zone 2) (fig 10).

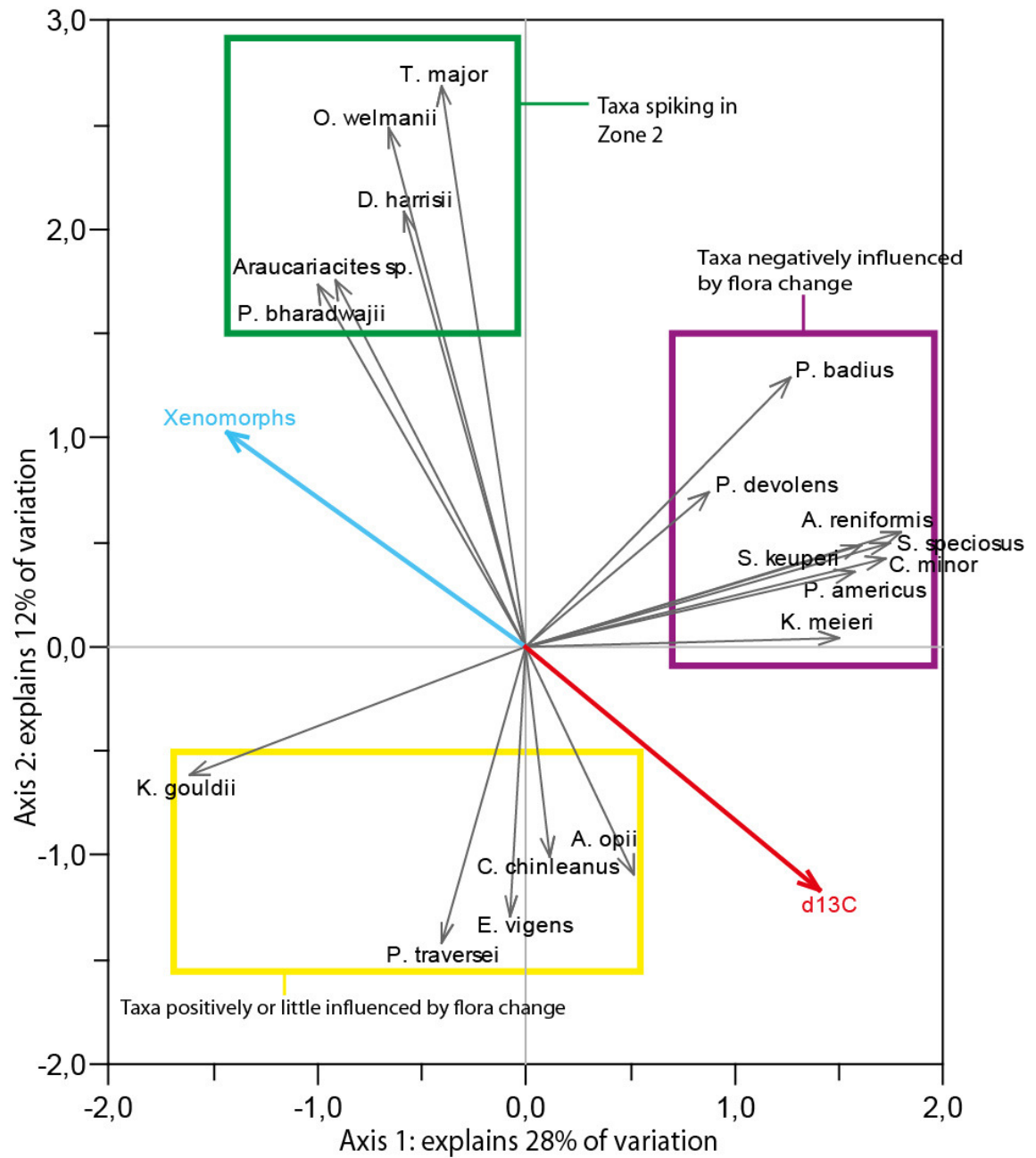


Figure 15: PCA plot with important groups. Note that a large number of species have been omitted from the plot.

Assessing possible causes

The most likely environmental factors influencing regional flora are temperature and humidity (e.g. Bonis et al., 2010). The increased spore taxa in Zone 2 might be indicative of humidity. From the data of the lithologically similar samples we see that $\delta^{13}\text{C}_{\text{TOC}}$ values become more positive from the Devil's Playground section into the Badlands section. Changing humidity could also have its effect on the $\delta^{13}\text{C}_{\text{TOC}}$ record, as the water brings in carbon from algae and/or carbon from upstream vegetation. From this data and moreover the large variance in the $\delta^{13}\text{C}_{\text{TOC}}$ record it is as yet impossible to say anything conclusive about the changing humidity, apart from the large scale climate change in the Late Triassic of North America, which is aridification (e.g. Dubiel et al., 1991; Prochnow et al., 2006; Cleveland et al., 2008).

Popularly, changes in $\delta^{13}\text{C}_{\text{TOC}}$ are often linked to changes in the isotopic composition of atmospheric CO_2 . It is possible that the change in $\delta^{13}\text{C}_{\text{TOC}}$ can be attributed to changes in the isotopic composition of atmospheric CO_2 . However, as our $\delta^{13}\text{C}_{\text{TOC}}$ record is quite sketchy and shows a lot of variance, more detailed research should be carried out to investigate any actual perturbances happening in the $\delta^{13}\text{C}_{\text{TOC}}$ record. If there would have been a perturbation in atmospheric CO_2 at the investigated interval, regional climatic belts would have shifted. An increase of CO_2 will have caused higher temperatures. Concerning the humidity, there are two possible scenarios: either the regional climate became drier, or possibly seasonality increased. This depends on how regional climate systems would respond to higher temperatures.

Popularly, mass extinctions are often linked to bolide or meteorite impacts. However, it seems unlikely that any of the five great mass extinctions of the Phanerozoic was caused solely by the impact of a bolide or meteorite. Even the environmental circumstances preceding the bolide impact at the Cretaceous-Paleogene boundary were already significantly stressful, the bolide impact merely represented the trigger of mass extinction (Glasby and Kunzendorf, 1996).

The Manicouagan impact in western Canada has been proposed as a trigger for mass extinction at the Triassic-Jurassic boundary, but was almost immediately rejected for the impact preceded the Triassic-Jurassic boundary by ~12.5 million year (Hodych and Dunning, 1992). The Manicouagan impact being timed at 214 Ma (± 2.5) (Walkden et al., 2002) and the Triassic-Jurassic boundary most recent dating puts it at 201.6 Ma (± 0.17) (Schaltegger et al., 2008).

The question remains if the Manicouagan impact was large enough to have an effect, regionally or globally. The Chicxulub crater, timed at exactly 65.5 Ma, has a radius of ~180 km (Hildebrand et al., 1991), whereas the Manicouagan crater is ~100 km in radius (Walkden et al., 2002). It is likely that an impact causing a crater of that magnitude should make its effects feel at least regionally, although the surface and the bedrock the bolide impacts also play a major role.

Extinction events are commonly associated with a short lived dominance of post disaster taxa or opportunistic pioneer vegetation. The Cretaceous-Paleogene boundary has a globally recognized spike in ferns, most likely caused by deforestation by the impact locally and the disappearance of many high light requiring canopy vegetation (e.g. Vajda et al., 2001). An impact half the size of the Chicxulub impact, such as the Manicouagan impact, would cause a similar trend in deforestation. A large deforestation near the impact (North America and western Eurasia) is likely to occur. Such a cataclysmic event would be followed by the diversification of opportunists or survivors from refugee areas.

The Manicouagan impact could be responsible for the turnover of vegetation within the Sonsela Member. However, there is no concrete evidence for this turnover occurring anywhere else but at Petrified Forest National Park, apart from undated palynofloral zonations

(e.g. Cornet, 1993, Cirilli, 2010). Moreover, the time frame only very roughly coincides as the Manicouagan impact has been timed at 214 Ma (± 2.5) and the only time constraints available at Petrified Forest National Park are datings of the Lower Blue Mesa Member at 219.2 Ma (± 0.7) (Martz and Parker, 2010) and the Black Forest bed (fig 2) at 211 Ma (± 0.7) (Riggs et al., 2003).

Conclusions and future research

Conclusions

The general trend of climate change in the Late Triassic of southwestern North America was aridification and increased temperatures. The mechanism for this change was the slow northwards movement of the continent from tropical latitudes to mid-latitudes and gradual outgassing caused by the opening of the Atlantic. The environmental circumstances governing at the investigated interval were semi-arid in the dominant upland environment, whereas in small patches of riparian lowlands tropical vegetation prevailed. The environment of southwestern North America was most likely subject to a highly seasonal climate at the investigated interval.

The transition between floral zone 2 and 3 erected by Litwin et al., (1991) has been constrained to an interval of two meters within the Jim Camp Wash beds. This interval also spans the faunal transition established by Parker and Martz (in press.). The rather abrupt change in fauna and flora occurring within the Sonsela Member of the Chinle Formation could suggest that within the Norian the gradual change in climate was interposed by an event, which caused the climate to change more sudden. The palynofloral record suggests the disappearance and decline of several pollen species and the dominance of an opportunist, *Klausipollenites gouldii*, which had to be well adapted to the stress of the environment. On a short lived interval there was an increase in spore taxa, which could be interpreted as high humidity tolerant and/or shade tolerant ferns. It remains to be investigated what triggered this turnover in vegetation.

The occurrence of xenomorphic structures in pollen and/or spores can be interpreted as indicators of environmental deterioration. As usually low abundance atmospheric components suddenly increase, it can cause mutagenesis in plants and in their reproductive cycles. The increase in xenomorphic structures occurring after the faunal turnover can be interpreted as a signal that a deterioration of atmospheric conditions took place at the same interval or was even the cause of the turnover.

Analyzing the data using Principal Components Analysis showed that the $\delta^{13}\text{C}_{\text{TOC}}$ was anti-correlated with the abundance of xenomorphic structures in *Klausipollenites gouldii*. This means that as $\delta^{13}\text{C}_{\text{TOC}}$ values decrease the amount of xenomorphic structures becomes higher. As the $\delta^{13}\text{C}_{\text{TOC}}$ record shows a lot of variance it is uncertain if we can draw any well established conclusions from this. Possibly changing atmospheric carbon abundances would influence regional temperature and humidity, which would have a direct influence on the vegetation.

We have established that with an uncertainty of ~2.3 meters a palynofloral turnover takes place within the same interval at which a faunal turnover takes place. Lithological evidence suggests that this event took place in a relative short amount of time. There are some signatures of a possible biotic crisis, e.g. the disappearance and decline of several taxa and the occurrence of a short lived increase in otherwise rare sporomorphs. A proposed mechanism for this turnover is the Manicouagan impact in Northeast Canada. However, the only evidence

for this is the very rough coincidence of the two events (an uncertainty of about 4 million years).

Future research

Data of floral and faunal investigations from Petrified Forest National Park suggest a substantial turnover occurring within the Sonsela Member. To explore the extent of this turnover more sections spanning the same interval should be investigated on palynoflora and vertebrate fauna. The main problem with investigating the extent of this change is correlating continental sections without absolute age constraints. Using palynofloral zones or vertebrate fauna zones, relative correlation can be approximated. However, the question remains if provincialism won't be of influence on the different records. If the turnover within the Sonsela Member has a greater extent it can be used as a stratigraphic marker.

The $\delta^{13}\text{C}_{\text{TOC}}$ record should be investigated to a greater extent. There is a large amount of uncertainty using the $\delta^{13}\text{C}_{\text{TOC}}$ in this case, because of the lack of sections with a similar or high enough amount of organic carbon. Using bulk $\delta^{13}\text{C}$ might prove more useful in lithological similar sections.

Climatic proxies can be investigated at high resolution at the interval of turnover to investigate how humidity and temperature were affected. This might also provide a more precise presumption of what important pollen and spore types, such as *Klausipollenites gouldii*, respond to. This way the occurrence of *K. gouldii* could be used as a biotic proxy.

Acknowledgements

First of all I'd like to thank Bill Parker and Jeff Martz for their help with setting up the project, ideas and fieldwork. Arnold van Dijk en Jan van Tongeren are acknowledged for their assistance in the laboratory, respectively with the carbon isotopes and the palynological samples. Sid Ash is acknowledged for his useful tips on cuticular analysis. I thank Wolfram Kürschner for putting me on the project, his tips on fieldwork and work in the field and guiding me towards the end result. I'd like to thank Wilma Wessels for her corrections, tips and strategies. Lastly I'd like to thank Han van Konijnenburg-van Cittert for her help, enthusiasm, tips and corrections.

References

- Alvin, K.L., 1982, Cheirolepidiaceae: biology, structure and palaeoecology: Review of palaeobotany and palynology, v. 37, p. 71-98.
- Ash, S.R., 1970a, *Dinophyton*, a problematic new plant genus from the Upper Triassic of the south-western United States: Palaeontology, v. 13, p. 646-663.
- , 1970b, *Pagiophyllum simpsonii*, a new conifer from the Chinle Formation (Upper Triassic) of Arizona: Journal of Paleontology, v. 44, p. 945-952.
- , 1972, Late Triassic plants from the Chinle Formation in Northeastern Arizona: Palaeontology, v. 15, p. 598-618.
- , 1973, Two new Late Triassic plants from the Petrified Forest of Arizona: Journal of Paleontology, v. 47, p. 46-53.

- , 1978, Plant megafossils, in Ash, S.R., ed. geology, paleontology and palaeoecology of a Late Triassic lake in western New Mexico: Brigham Young University Geology Studies, v. 25, p. 23-43.
- , 1980, Upper Triassic floral zones of North America: *In* D.L. Dichler and T.M Taylor (eds.), Biostratigraphy of fossil plants, v. 1, p. 153-270.
- , 1987, Growth habits and systematics of the Upper Triassic plant *Pelourdea poleoensis*, southwestern USA: Review of Palaeobotany and Palynology, v. 51, p. 37-49.
- , 1999, An Upper Triassic upland flora from north-central New Mexico, USA: Review of palaeobotany and palynology, v. 105, p. 183-199.
- , 2001, New Cycadophytes from the Upper Triassic Chinle Formation of the southwestern United States: *PaleoBios*, v. 21, p. 15-28.
- Ash, S.R., and Creber, G.T., 1992, Palaeoclimatic interpretation of the wood structures of the trees in the Chinle Formation (Upper Triassic), Petrified Forest National Park, Arizona, USA: *Palaeogeography, Palaeoclimatology, Palaeoecology*, v. 96, p. 299-317.
- Ash, S.R., and Litwin, R.J., 1996, Two new species of the pinnate microsporophyll *Pramelreuthia* from the Upper Triassic of the southwestern United States: *American Journal of Botany*, v. 83, p. 1091-1099.
- Balme, B.E., 1970, Palynology of Permian and Triassic strata in the Salt Range and Surghar Range, West Pakistan: University of Kansas Department of Geology Special Publications, v. 4, p. 306-453.
- , 1995, Fossil in situ spores and pollen grains: an annotated catalogue: *Palaeobotany and palynology*, v. 87, p. 81-323.
- Benton, M.J., 1986, More than one event in the Late Triassic mass extinction: *Nature*, v. 321, p. 857-861.
- Bonis, N.R., 2010, Palaeoenvironmental changes and vegetation history during the Triassic-Jurassic transition: Utrecht University doctoral dissertation, p. 216.
- Bonis, N.R., Ruhl, M., and Kürschner, W.M., 2010, Milankovitch-scale palynological turnover across the Triassic Jurassic transition at St. Audries Bay, SW UK: *Journal of the Geological Society*, v. 167, p. 877-888.
- Boutton, T.W., 1991, Stable carbon isotope ratios of natural materials: II. Atmospheric, terrestrial, marine and freshwater environments. In: D.C. Coleman and B. Fry, editors. *Carbon Isotope Techniques*. Academic press, San Diego, California, USA. p. 173-185.
- Cirilli, S., 2010, Upper Triassic and Lowermost Jurassic palynology and palynostratigraphy: a review: *Geological Society of London: Special Publications*, v. 334, p. 285-314.
- Cleveland, D.M., Nordt, L.C., and Atchley, S.C., 2008, Paleosols, trace fossils, and precipitation estimates of the uppermost Triassic strata in northern New Mexico: *Palaeogeography, Palaeoclimatology, Palaeoecology*, v. 257, p. 421-444.
- Cornet, B., 1977, Preliminary investigation of two Late Triassic conifers from York County, Pennsylvania: In: R.C. Romans (Editor), *Geobotany*. Plenum, New York, v. 1, p. 165-172.
- , 1993, Applications and limitations of palynology in age, climatic, and paleoenvironmental analyzes of Triassic sequences in North America: *New Mexico Museum of Natural History & Science Bulletin*, v. 3, p. 75-93.
- Daugherty, L.H., 1941, The Upper Triassic flora of Arizona: Carnegie Institution of Washington Publication, v. 526, p. 108.
- Demko, T.M., Dubiel, R.F., and Parrish, J.T., 1998, Plant taphonomy in incised valleys: Implications for interpreting paleoclimate from fossil plants: *Geology*, v. 26, p. 1119-1122.

- Dolby, J.H., and Balme, B.E., 1976, Triassic palynology of the Carnarvon Basin, Western Australia: Review of palaeobotany and palynology, v. 22, p. 105-168.
- Dubiel, R.F., Parrish, J.T., Parrish, J.M., and Good, S.C., 1991, The Pangaeon megamonsoon - evidence from the Upper Triassic Chinle Formation, Colorado Plateau: *Palaios*, v. 6, p. 347-370.
- Dunay, R.E., and Fisher, M.J., 1979, Palynology of the Dockum Group (Upper Triassic), Texas, U.S.A.: Review of palaeobotany and palynology, v. 28, p. 61-92.
- Farjon, A., 2008, A natural history of conifers: Timber Press.
- Fisher, M.J., and Dunay, R.E., 1984, Palynology of the Petrified Forest Member of the Chinle Formation (Upper Triassic), Arizona, U.S.A: *Pollen et Spores*, v. 26, p. 241-284.
- Foster, C.B., and Afonin, S.A., 2005, Abnormal pollen grains: an outcome of deteriorating atmospheric conditions around the Permian-Triassic boundary: *Journal of the Geological Society, London*, v. 162, p. 653-659.
- Furin, S., Preto, N., Rigo, M., Roghi, G., Gianolla, P., Crowley, J.L., and Bowering, S.A., 2006, High-precision U-Pb zircon age from the Triassic of Italy: Implications for the Triassic time scale and the Carnian origin of calcareous nannoplankton and dinosaurs: *Geology*, v. 34, p. 1009-1012.
- Glasby, G.P., and Kunzendorf, H., 1996, Multiple factors in the origin of the Cretaceous/Tertiary boundary: the role of environmental stress and Deccan Trap volcanism: *Geologische Rundschau*, v. 85, p. 191-210.
- Heckert, A.B., and Lucas, S.G., 2002, Revised Upper Triassic stratigraphy of the Petrified Forest National Park, Arizona, U.S.A: *New Mexico Museum of Natural History and Science Bulletin*, v. 21, p. 37-42.
- Heckert, A.B., Lucas, S.G., Hunt, A.P., and Spielmann, J.A., 2007, Late Triassic Aetosaur biochronology revisited: *New Mexico Museum of Natural History & Science Bulletin*, v. 41, p. 49-50.
- Hesselbo, S.P., Robinson, S.A., Surlyk, F., and Piasecki, S., 2002, Terrestrial and marine extinction at the Triassic-Jurassic boundary synchronized with major carbon-cycle perturbation: a link to initiation of massive volcanism?: *Geology*, v. 30, p. 251-254.
- Hildebrand, A.R., Penfield, G.T., Kring, D.A., Pilkington, M., Camargo, Z.A., Jacobsen, S.B., and Boynton, W.V., 1991, Chicxulub Crater: A possible Cretaceous/Tertiary boundary impact crater on the Yucatán Peninsula, Mexico: *Geology*, v. 19, p. 867-871.
- Hodych, J.P., and Dunning, G.R., 1992, Did the Manicouagan impact trigger the end-of-Triassic mass extinction?: *Geology*, v. 20, p. 51-54.
- Jansonius, J., 1962, Palynology of Permian and Triassic sediments, Peace River Area, Western Canada: *Palaeonographica*, v. 110, p. 35-98.
- Kerp, H., 1990, The study of fossil gymnosperms by means of cuticular analysis: *Palaios*, v. 5, p. 548-569.
- Kirkland, D.W., and Frederiksen, N.O., 1970, *Cordaitina* pollen from Pennsylvanian strata of Oklahoma and Texas: Review of palaeobotany and palynology, v. 10, p. 221-231.
- Klaus, W., 1964, Für Bohr- und fördertechnik gewinnung, aufbereitung, transport: *Erdoel*, v. 80, p. 119-132.
- Leschik, G., 1956, Die Keuperflora von Neuwelt bei Basel: *Schweizerische Palaeontologische Abhandlungen*, v. 72, p. 1-70.
- Litwin, R.J., 1986, The palynostratigraphy and age of the Chinle and Moenave Formations, southwestern U.S.A.: Diss., Pennsylvania State Univ., University Park., p. 265.
- Litwin, R.J., Traverse, A., and Ash, S.R., 1991, Preliminary palynological zonation of the Chinle Formation, southwestern U.S.A., and its correlation to the Newark Supergroup (eastern U.S.A.): *Palaeobotany and palynology*, v. 68, p. 269-287.

- Litwin, R.J., Smoot, J.P., and Weems, R.E., 1993, *Froelichsporites* gen. nov. - A biostratigraphic marker palynomorph of Upper Triassic continental strata in the conterminous U.S.: *Palynology*, v. 17, p. 157-168.
- Mädler, K., 1964, Die geologische Verbreitung von Sporen und Pollen in der Deutschen Trias: Beihefte zum Geologischen Jahrbuch, v. 65, p. 1-147.
- Martz, J.W., and Parker, W.G., 2010, Revised lithostratigraphy of the Sonsela Member (Chinle Formation, Late Triassic) in the southern part of Petrified Forest National Park, Arizona: *PLoS One*, v. 5, p. 1-26.
- Marzoli, A., Renne, P.R., Piccirillo, E.M., Ernesto, M., Bellieni, G., and De Min, A., 1999, Extensive 200-million year old continental flood basalts of the Central Atlantic Magmatic Province: *Science*, v. 284, p. 616-618.
- Murry, P.A., 1990, Stratigraphy of the Upper Triassic Petrified Forest Member (Chinle Formation) in Petrified Forest National Park, Arizona, USA: *Journal of Geology*, v. 98, p. 780-789.
- Murry, P.A., and Long, R.A., 1989, Geology and paleontology of the Chinle Formation, Petrified Forest National Park and vicinity, Arizona, and a discussion of vertebrate fossils of the southwestern Upper Triassic: In: Lucas SG, Hunt AP, eds. Dawn of the Age of Dinosaurs in the American Southwest. Albuquerque: New Mexico Museum of Natural History, p. 29-64.
- Muttoni, G., Kent, D.V., Olsen, P.E., Di Stefano, P., Lowrie, W., Bernasconi, S.M., and Martín Hernández, F., 2004, Tethyan magnetostratigraphy from Pizzo Mondello (Sicily) and correlation to the Late Triassic Newark astrochronological polarity time scale: *Geological Society of America Bulletin*, v. 116, p. 1043-1058.
- Nilsson, T., 1958, Über das Vorkommen eines Mesozoischen Sapropelgesteins in Schonen: *Lunds Universitets Årsskrift*, v. 54, p. 1-126.
- Parker, W.G., 2006, The stratigraphic distribution of major fossil localities in Petrified Forest National Park, Arizona: *Museum of Northern Arizona Bulletin*, v. 62, p. 46-61.
- Parker, W.G. and Martz, J.W., in press, Constraining the stratigraphic position of the Late Triassic (Norian) Adamanian-Revueltian faunal transition in the Chinle Formation of Petrified Forest National Park, Arizona: *Earth and Environmental Transactions of the Royal Society of Edinburgh*, v. -, p. -.
- Pautsch, M.E., 1973, Upper Triassic spores and pollen from the Polish Carpathian Foreland: *Micropaleontology*, v. 19, p. 129-149.
- Prochnow, S.J., Nordt, L.C., Atchley, S.C., and Hudec, M.R., 2006, Multi-proxy paleosol evidence for middle and late Triassic climate trends in eastern Utah: *Palaeogeography, Palaeoclimatology, Palaeoecology*, v. 232, p. 53-72.
- Riggs, N.R., Ash, S.R., Barth, A.P., Gehrels, G.E., and Wooden, J.L., 2003, Isotopic age of the Black Forest Bed, Petrified Forest Member, Chinle Formation, Arizona: An example of dating a continental sandstone: *GSA Bulletin*, v. 115, p. 1315-1323.
- Ruhl, M., Bonis, N.R., Reichart, G.-J., Sinninghe Damsté, J., and Kürschner, W., in prep., Atmospheric methane injection caused end-Triassic mass extinction: *Science*, v. -, p. -.
- Ruhl, M., Kürschner, W.M. and Krystyn, L., 2009, Triassic–Jurassic organic carbon isotope stratigraphy of key sections in the western Tethys realm (Austria): *Earth and Planetary Science Letters*, v. 281, p. 169-187.
- Schaltegger, U., Guex, J., Bartolini, A., Schoene, B., and Ovtcharova, M., 2008, Precise U-Pb age constraints for end-Triassic mass extinction, its correlation to volcanism and Hettangian post-extinction recovery: *Earth and Planetary Science Letters*, v. 267, p. 266-275.

- Scheuring, B.W., 1970, Palynologische und palynostratigraphische Untersuchungen des Keupers im Bölchentunnel (Solothurner Jura): Schweizerische Paläontologische Abhandlungen, v. 88, p. 119.
- Sephton, M.A., Amor, K., Franchi, I.A., Wignall, P.B., Newton, R.J., and Zonneveld, J.-P., 2002, Carbon and nitrogen isotope disturbances and an end-Norian (late Triassic) extinction event: *Geology*, v. 30, p. 1119-1122.
- Tanner, L.H., Lucas, S.G., and Chapman, M.G., 2004, Assessing the record and causes of Late Triassic extinctions: *Earth-science reviews*, v. 65, p. 103-139.
- Vajda, V., Raine, J.I., and Hollis, C.J., 2001, Indication of global deforestation at the Cretaceous-Tertiary boundary by New Zealand fern spike: *Science*, v. 294, p. 1700-1702.
- Visscher, H., 1966, Palaeobotany of the Mesophytic III: Plant microfossils from the Upper Bunter of Hengelo, the Netherlands: *Acta Botanica Neerlandica*, v. 15, p. 316-375.
- Visscher, H., Looy, C.V., Collinson, M.E., Brinkhuis, H., van Konijnenburg-van Cittert, J.H.A., Kürschner, W., and Sephton, M.A., 2004, Environmental mutagenesis during the end-Permian ecological crisis: *Proceedings of the National Academy of Sciences of the USA*, v. 101, p. 12952–12956.
- Walkden, G., Parker, J., and Kelley, S., 2002, A Late Triassic impact ejecta layer in southwestern Britain: *Science*, v. 298, p. 2185-2188.
- Zavialova, N.E., and Roghi, G., 2005, Exine morphology and ultrastructure of *Duplicisporites* from the Triassic of Italy: *Grana*, v. 44, p. 337-342.

APPENDIX A

PLATE 1

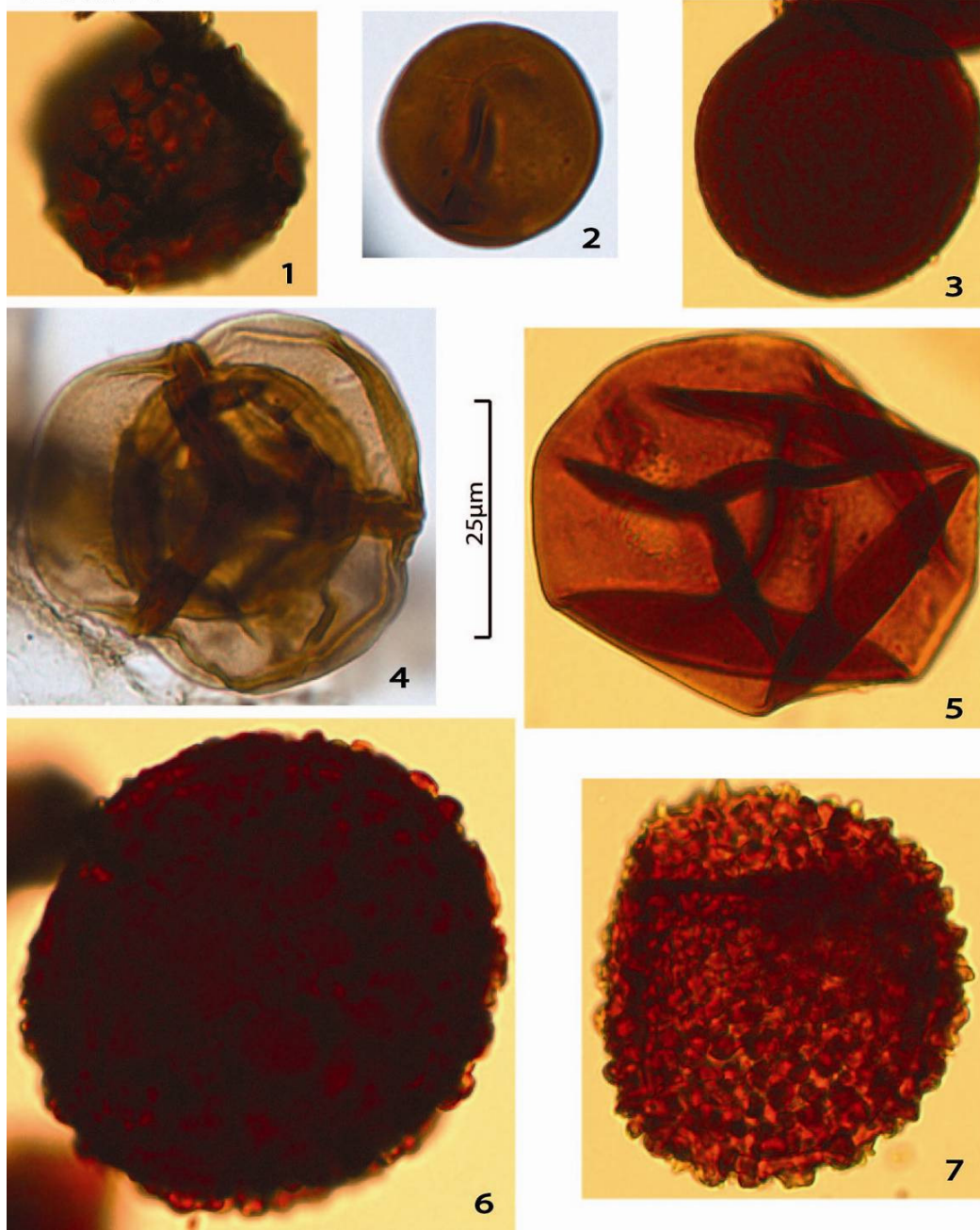


Plate 1:

- 1: *Convolutispora klukiforma*, DP3-3, 30.9/109.9
- 2: *Todisporite minor*; monolete, BL2-15, 60.1/97.0
- 3: ? *Osmundacidites wellmannii*, BL5-1, 52.8/111.5
- 4: *Froelichsporites traversei*, BL2-3, 54.6/109.1
- 5: *Todisporites major*, BL5-12, 55.7/94.2
- 6: *Foveolatitriteles potonieii*, DP2-7, 34.9/99.7
- 7: *Trilites klausii*, BL5-11, 53.1/95.5

PLATE 2

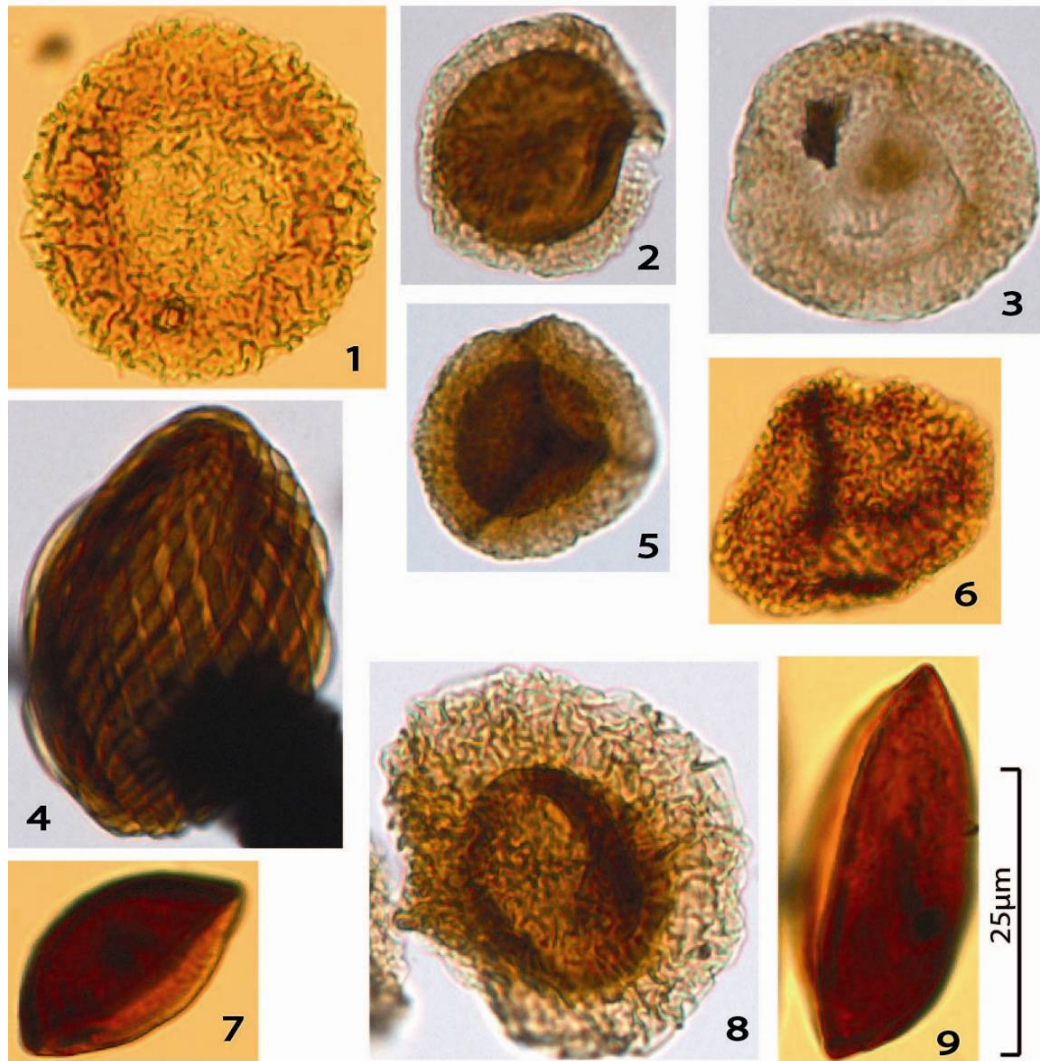


Plate 2:

- 1: *Patinasporites densus*, BL5-3, 59.9/107.3
- 2: *Kuglerina meieri*, DP3-5, 46.6/108.2
- 3: *Cordaitina minor*, DP3-12, 46.1/105.3
- 4: *Equisetosporites chinleanus*, DP2-9, 46.4/106.5
- 5: *Tulesporites terraerubrae*, BL2-14, 56.0/100.0
- 6: *Vallasporites ignacii*, BL1-3, 50.8/103.4
- 7: *Cycadopites fragilis*, BL5-10, 50.9/100.1
- 8: *Heliosaccus dimorphus*, DP3-2, 30.9/109.7
- 9: *Cycadopites follicularis*, BL5-8, 57.8/104.4

PLATE 3

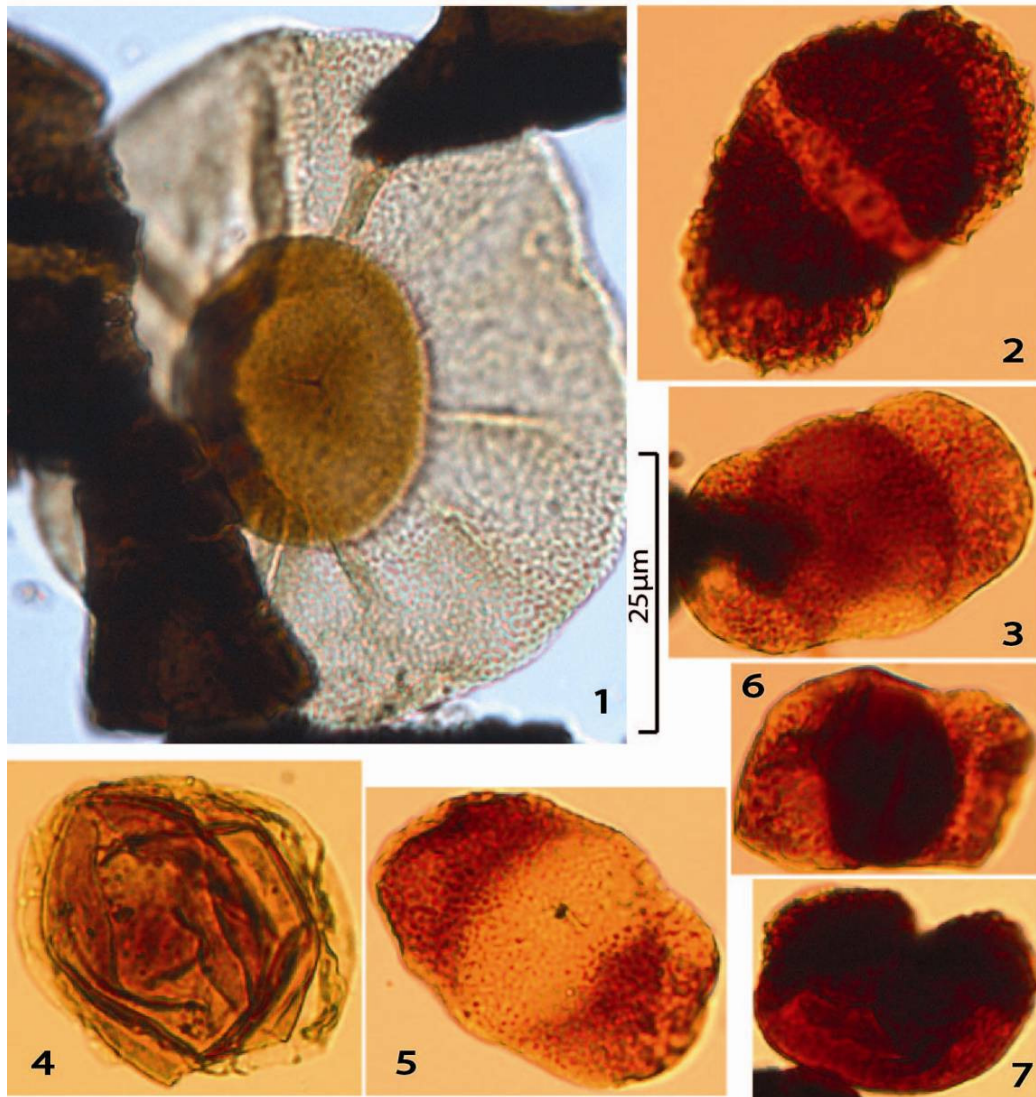


Plate 3:

- 1: *Guthoerlisporites cancellous*, BL5-14, 54.5/105.5
- 2: *Plicatisaccus badius*, DP2-1, 41.1/94.5
- 3: *Triadispora fallax*, DP1-5, 23.4/107.2
- 4: *Araucariacites* sp., BL5-2, 57.9/111.3
- 5: *Klausipollenites gouldii* (type B1), DP1-1, 37.1/99.7
- 6: *Triadispora dockumensis*, DP1-13, 27.7/94.2
- 7: *Minutosaccus crenulatus*, DP1-7, 38.2/107.1

PLATE 4

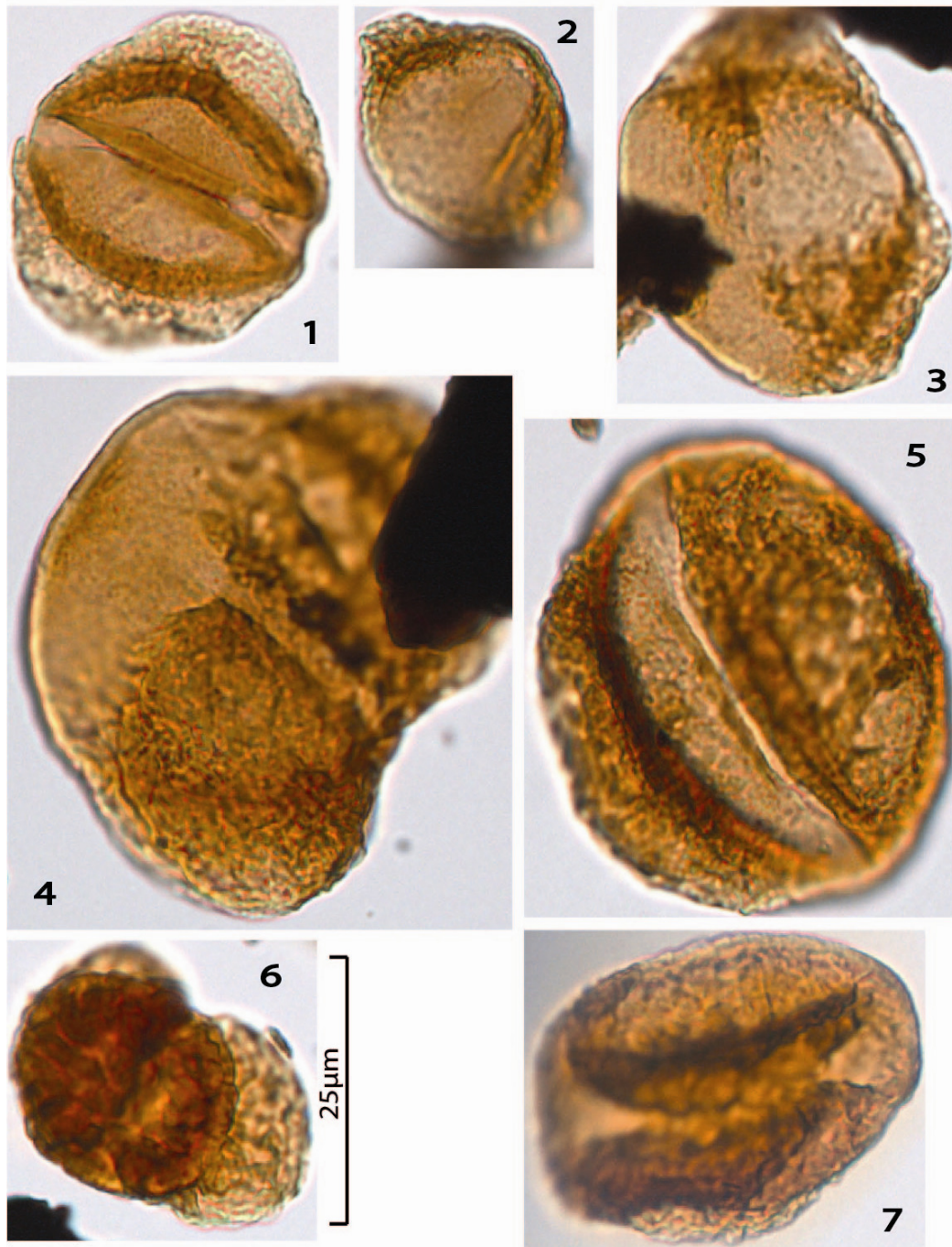


Plate 4:

- 1: *Protodiploxypinus americus*, DP3-15, 34.9/103.3
- 2: *Protodiploxypinus ujhelyi*, DP2-10, 33.2/106.5
- 3: *Protodiploxypinus fastidiosus*, DP3-10, 42.0/106.6
- 4: *Protodiploxypinus lacertosus*, DP3-11, 42.0/105.4
- 5: *Angustisaccus reniformis*, DP3-6, 39.6/107.3
- 6: *Pseudillinites crassus*, DP3-1, 34.0/109.7
- 7: *Angustisaccus petulans*, DP3-13, 45.2/104.9

PLATE 5

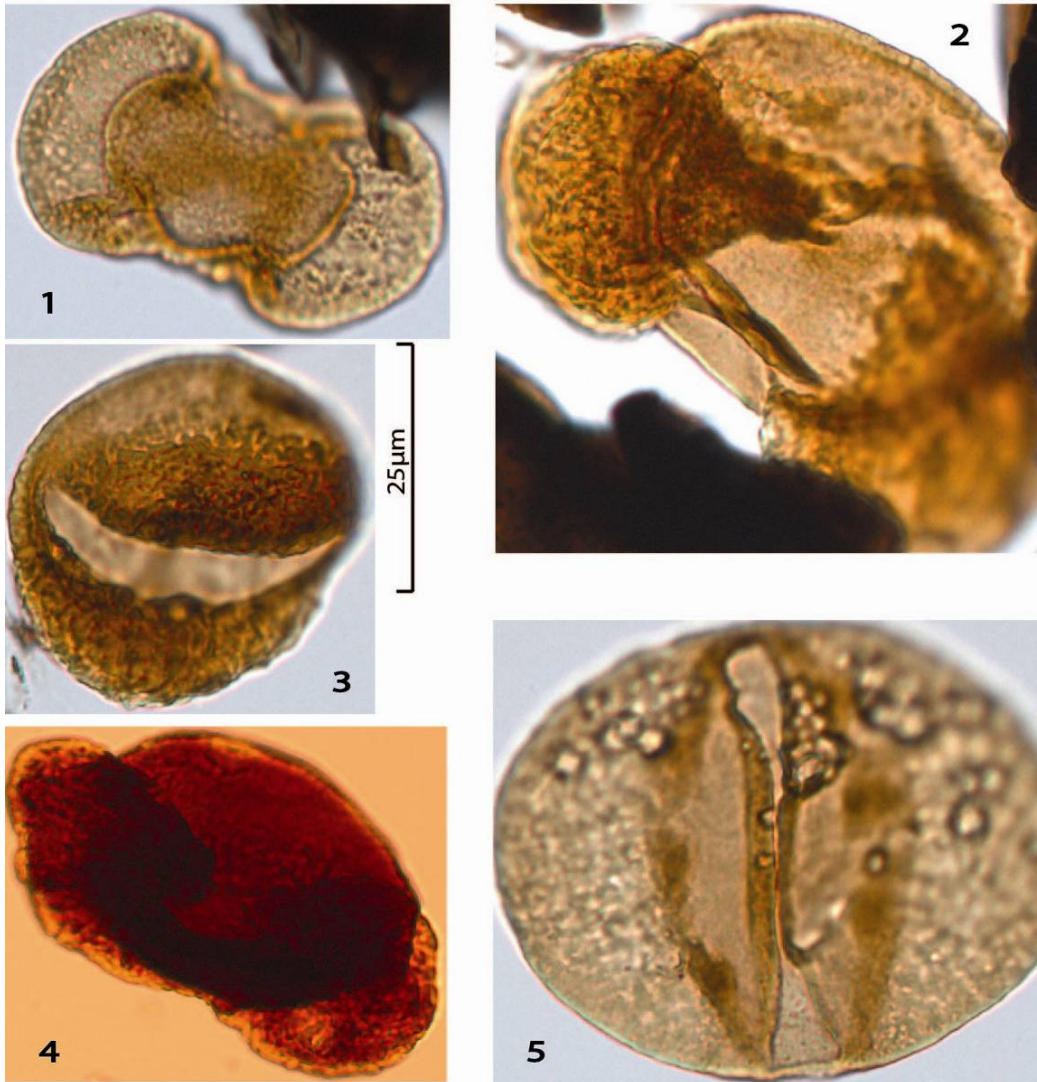


Plate 5:

- 1: *Platysaccus triassicus*, BL2-1, 59.3/110.4
- 2: *Pityosporites devolens*, BL2-7, 52.1/108.4
- 3: *Schizosaccus keuperi*, BL2-12, 57.6/100.9
- 4: *Samaropollenites speciosus*, DP1-4, 26.4/105.1
- 5: *Falcisporites gottesfeldi*, BL2-13, 55.5/100.8

PLATE 6

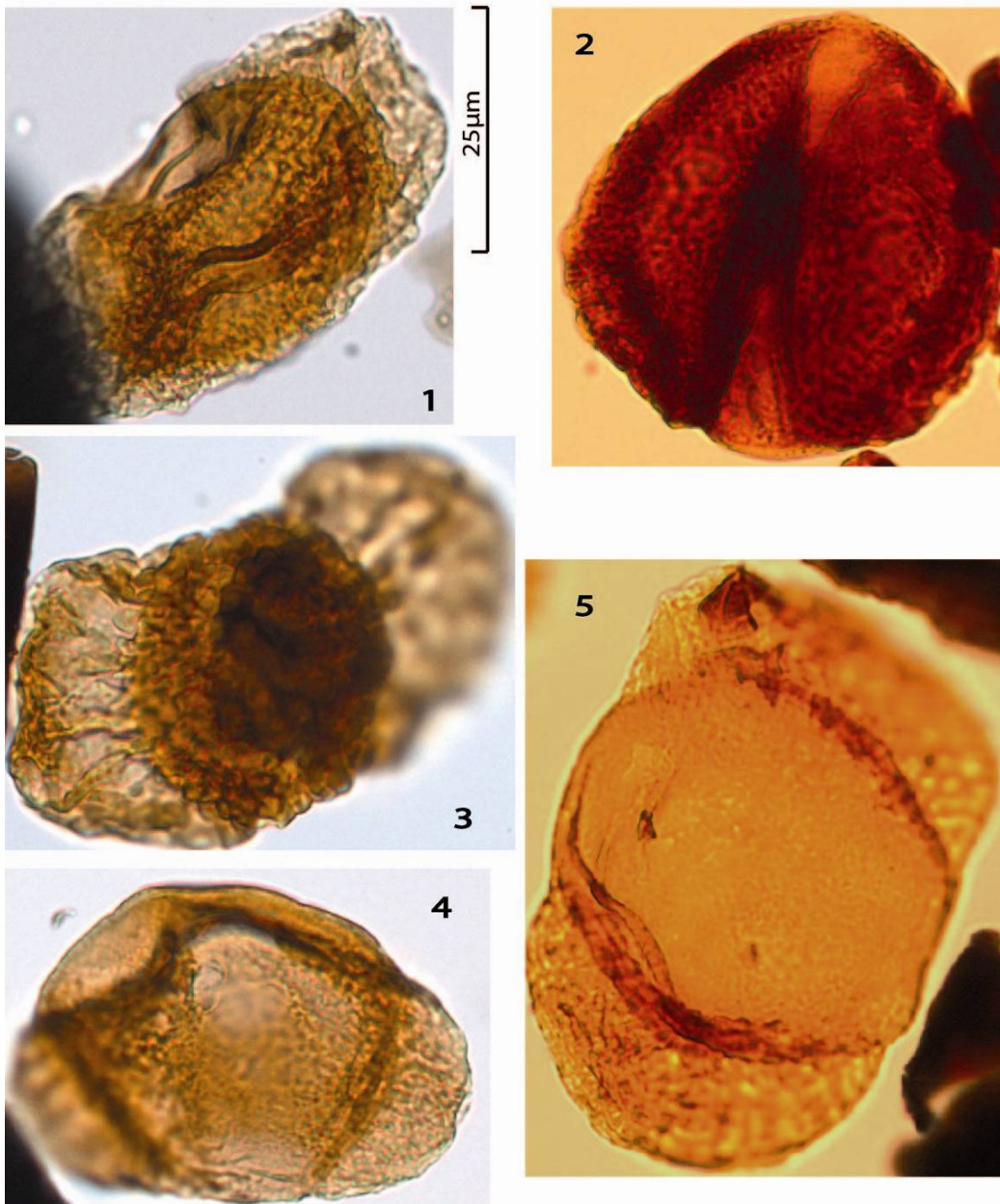


Plate 6:

- 1: *Chordasporites chinleanus*, DP4-3, 34.5/110.5
- 2: *Sulcatisporites krauselii*, DP1-6, 26.5/107.1
- 3: *Rugubivesiculites proavitus*, BL2-2, 57.4/109.8
- 4: *Klausipollenites schaubergeri*, DP3-3, 30.9/109.9
- 5: *Voltziaceasporites heteromorpha*, DP2-5, 43.7/95.5

PLATE 7

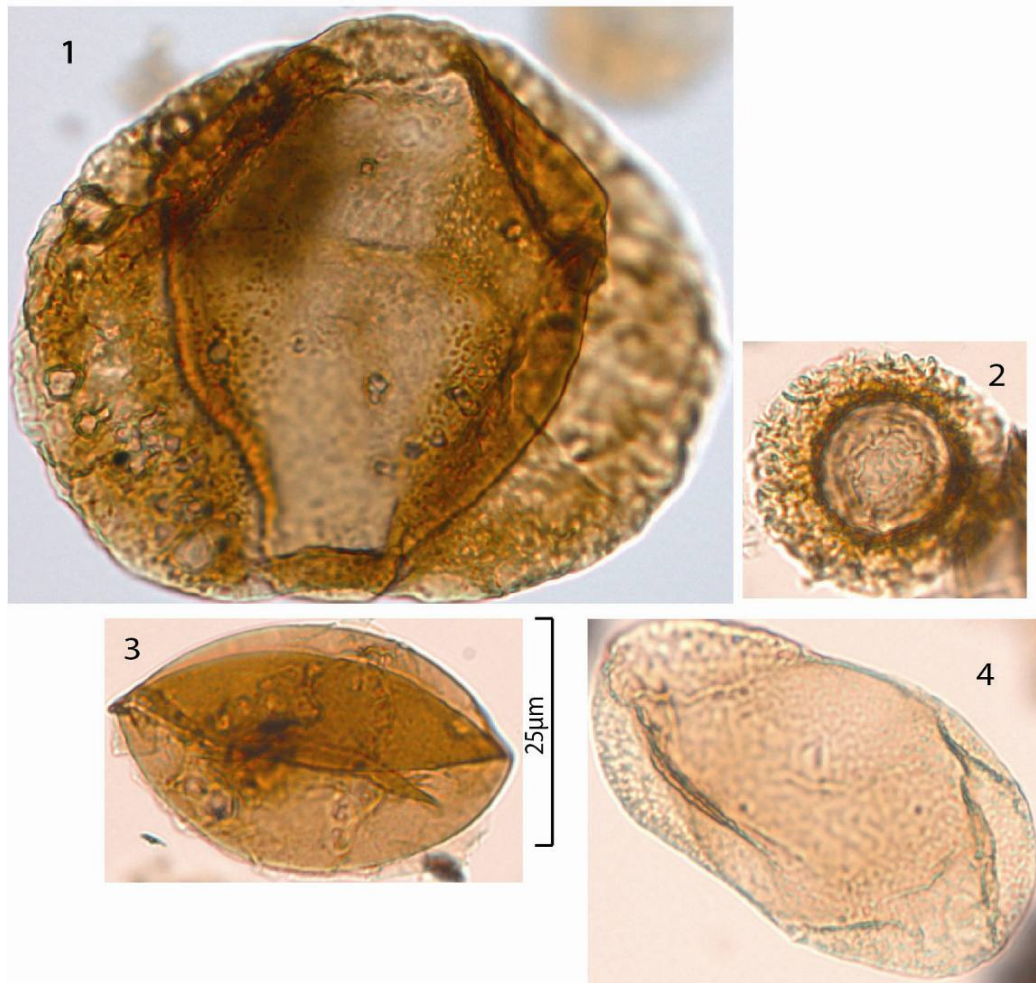
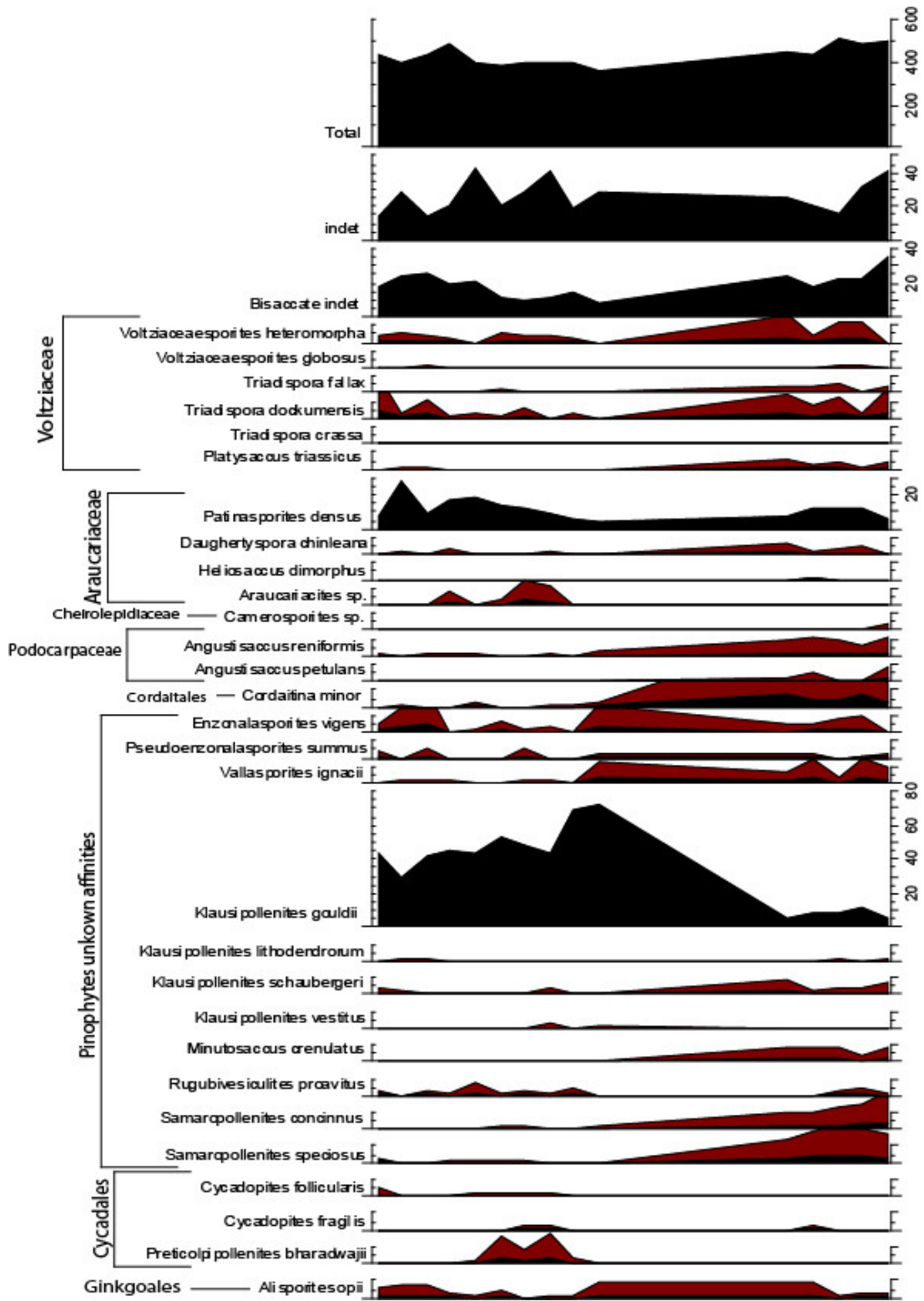
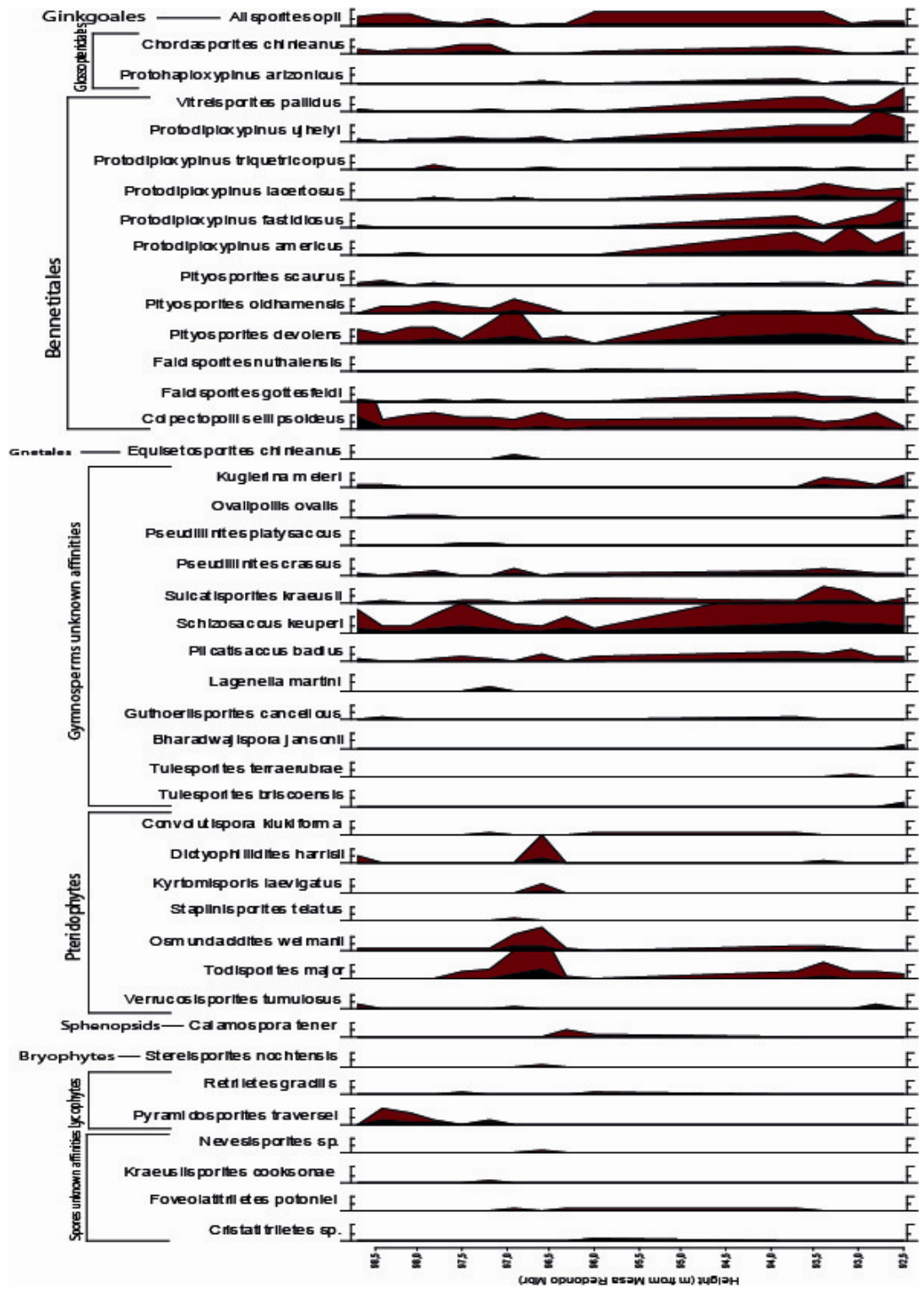


Plate 7:

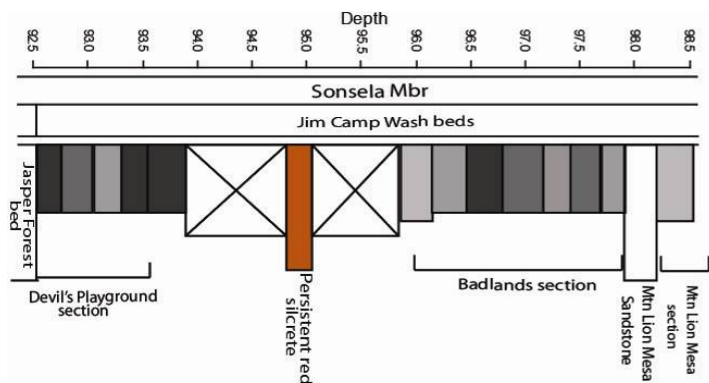
- 1: *Alisporites opii*, BL2-16, 61.8/102.5
- 2: *Daughertyspora chinleana*, BL6-1, 46.8/99.3
- 3: *Preticolpipollenites bharadwajii*, BL6-2, 46.3/99.4
- 4: *Colpectopollis ellipsoideus*, MLM3-1, 60.5/100.1

APPENDIX B





APPENDIX C



Depth	925	930	935	940	945	950	955	960	965	970	975	980	985	Species
●	●	●	●	●	●	●	●	●	●	●	●	●	●	<i>Alisporites opii</i>
●	●	●	●	●	●	●	●	●	●	●	●	●	●	<i>Angustisaccus petulans</i>
●	●	●	●	●	●	●	●	●	●	●	●	●	●	<i>Angustisaccus reniformis</i>
●	●	●	●	●	●	●	●	●	●	●	●	●	●	<i>Araucariacites sp.</i>
●	●	●	●	●	●	●	●	●	●	●	●	●	●	<i>Bharadwajispora jansonii</i>
●	●	●	●	●	●	●	●	●	●	●	●	●	●	<i>Calamospora tener</i>
●	●	●	●	●	●	●	●	●	●	●	●	●	●	<i>Camerospores sp.</i>
●	●	●	●	●	●	●	●	●	●	●	●	●	●	<i>Chordasporites chinleanus</i>
●	●	●	●	●	●	●	●	●	●	●	●	●	●	<i>Cirratiradites sp.</i>
●	●	●	●	●	●	●	●	●	●	●	●	●	●	<i>Colpectopollis ellipsoideus</i>
●	●	●	●	●	●	●	●	●	●	●	●	●	●	<i>Conbaculatisporites sp.</i>
●	●	●	●	●	●	●	●	●	●	●	●	●	●	<i>Convolutispora klukiforma</i>
●	●	●	●	●	●	●	●	●	●	●	●	●	●	<i>Cordaitina minor</i>
●	●	●	●	●	●	●	●	●	●	●	●	●	●	<i>Cristatiriletes sp.</i>
●	●	●	●	●	●	●	●	●	●	●	●	●	●	<i>Cycadopites follicularis</i>
●	●	●	●	●	●	●	●	●	●	●	●	●	●	<i>Cycadopites fragilis</i>
●	●	●	●	●	●	●	●	●	●	●	●	●	●	<i>Cycadopites stonei</i>
●	●	●	●	●	●	●	●	●	●	●	●	●	●	<i>Daughertyspora chinleana</i>
●	●	●	●	●	●	●	●	●	●	●	●	●	●	<i>Dictyophillidites harrisii</i>
●	●	●	●	●	●	●	●	●	●	●	●	●	●	<i>Duplicisporites granulatus</i>
●	●	●	●	●	●	●	●	●	●	●	●	●	●	<i>Enzonasporites vigens</i>
●	●	●	●	●	●	●	●	●	●	●	●	●	●	<i>Equisetosporites chinleanus</i>
●	●	●	●	●	●	●	●	●	●	●	●	●	●	<i>Falcisporites gottesfeldi</i>
●	●	●	●	●	●	●	●	●	●	●	●	●	●	<i>Falcisporites nuthalensis</i>
●	●	●	●	●	●	●	●	●	●	●	●	●	●	<i>Foveolatisporites potonieii</i>
●	●	●	●	●	●	●	●	●	●	●	●	●	●	<i>Granulatisporites infirmus</i>
●	●	●	●	●	●	●	●	●	●	●	●	●	●	<i>Guthoerlisporites cancellous</i>
●	●	●	●	●	●	●	●	●	●	●	●	●	●	<i>Heliosaccus dimorphus</i>
●	●	●	●	●	●	●	●	●	●	●	●	●	●	<i>Infernopollenites sp.</i>
●	●	●	●	●	●	●	●	●	●	●	●	●	●	<i>Klausipollenites gouldii</i>
●	●	●	●	●	●	●	●	●	●	●	●	●	●	<i>Klausipollenites lithodendrorum</i>
●	●	●	●	●	●	●	●	●	●	●	●	●	●	<i>Klausipollenites schaubergeri</i>
●	●	●	●	●	●	●	●	●	●	●	●	●	●	<i>Klausipollenites vestitus</i>
●	●	●	●	●	●	●	●	●	●	●	●	●	●	<i>Klukisporites granosifene-stellatus</i>
●	●	●	●	●	●	●	●	●	●	●	●	●	●	<i>Kraeuslisporites cooksonae</i>
●	●	●	●	●	●	●	●	●	●	●	●	●	●	<i>Kuglerina meieri</i>
●	●	●	●	●	●	●	●	●	●	●	●	●	●	<i>Kyrtomsporites laevigatus</i>
●	●	●	●	●	●	●	●	●	●	●	●	●	●	<i>Lagenella martini</i>
●	●	●	●	●	●	●	●	●	●	●	●	●	●	<i>Minutosaccus crenulatus</i>
●	●	●	●	●	●	●	●	●	●	●	●	●	●	<i>Nevesisporites sp.</i>
●	●	●	●	●	●	●	●	●	●	●	●	●	●	<i>Osmundacidites wellmannii</i>
●	●	●	●	●	●	●	●	●	●	●	●	●	●	<i>Ovalipollis ovalis</i>
●	●	●	●	●	●	●	●	●	●	●	●	●	●	<i>Patinasporites densus</i>
●	●	●	●	●	●	●	●	●	●	●	●	●	●	<i>Pityosporites devolens</i>
●	●	●	●	●	●	●	●	●	●	●	●	●	●	<i>Pityosporites oldhamensis</i>
●	●	●	●	●	●	●	●	●	●	●	●	●	●	<i>Pityosporites scaurus</i>
●	●	●	●	●	●	●	●	●	●	●	●	●	●	<i>Platysaccus triassicus</i>
●	●	●	●	●	●	●	●	●	●	●	●	●	●	<i>Plicatisaccus badius</i>
●	●	●	●	●	●	●	●	●	●	●	●	●	●	<i>Preticolpipo-pollenites bharadwajii</i>
●	●	●	●	●	●	●	●	●	●	●	●	●	●	<i>Protodiploxy-pinus americus</i>
●	●	●	●	●	●	●	●	●	●	●	●	●	●	<i>Protodiploxy-pinus fastidiosus</i>
●	●	●	●	●	●	●	●	●	●	●	●	●	●	<i>Protodiploxy-pinus lacertosus</i>
●	●	●	●	●	●	●	●	●	●	●	●	●	●	<i>Protodiploxy-pinus triquetricorpus</i>
●	●	●	●	●	●	●	●	●	●	●	●	●	●	<i>Protodiploxy-pinus ujhelyi</i>
●	●	●	●	●	●	●	●	●	●	●	●	●	●	<i>Protohaploxy-pinus arizonicus</i>
●	●	●	●	●	●	●	●	●	●	●	●	●	●	<i>Pseudoenzonalasporites summus</i>
●	●	●	●	●	●	●	●	●	●	●	●	●	●	<i>Pseudollinities crassus</i>
●	●	●	●	●	●	●	●	●	●	●	●	●	●	<i>Pseudollinities platysaccus</i>
●	●	●	●	●	●	●	●	●	●	●	●	●	●	<i>Pyramidosporites traversei</i>
●	●	●	●	●	●	●	●	●	●	●	●	●	●	<i>Retriletes gracilis</i>
●	●	●	●	●	●	●	●	●	●	●	●	●	●	<i>Rugubivesiculites proavitus</i>
●	●	●	●	●	●	●	●	●	●	●	●	●	●	<i>Samaropollenites concinnus</i>
●	●	●	●	●	●	●	●	●	●	●	●	●	●	<i>Samaropollenites speciosus</i>
●	●	●	●	●	●	●	●	●	●	●	●	●	●	<i>Schizosaccus keuperi</i>
●	●	●	●	●	●	●	●	●	●	●	●	●	●	<i>Staplinisporites telatus</i>
●	●	●	●	●	●	●	●	●	●	●	●	●	●	<i>Stereisporites noctentis</i>
●	●	●	●	●	●	●	●	●	●	●	●	●	●	<i>Sulcatisporites krauselii</i>
●	●	●	●	●	●	●	●	●	●	●	●	●	●	<i>Todisporites major</i>
●	●	●	●	●	●	●	●	●	●	●	●	●	●	<i>Triadispora crassa</i>
●	●	●	●	●	●	●	●	●	●	●	●	●	●	<i>Triadispora dockumensis</i>
●	●	●	●	●	●	●	●	●	●	●	●	●	●	<i>Triadispora fallax</i>
●	●	●	●	●	●	●	●	●	●	●	●	●	●	<i>Trilites klausii</i>
●	●	●	●	●	●	●	●	●	●	●	●	●	●	<i>Tulesporites briscoensis</i>
●	●	●	●	●	●	●	●	●	●	●	●	●	●	<i>Tulesporites terraerubrae</i>
●	●	●	●	●	●	●	●	●	●	●	●	●	●	<i>Vallasporites ignacii</i>
●	●	●	●	●	●	●	●	●	●	●	●	●	●	<i>Verrucosporites tumulosus</i>
●	●	●	●	●	●	●	●	●	●	●	●	●	●	<i>Vitreisporites pallidus</i>
●	●	●	●	●	●	●	●	●	●	●	●	●	●	<i>Voltziaceasporites globosus</i>
●	●	●	●	●	●	●	●	●	●	●	●	●	●	<i>Voltziaceasporites heteromorpha</i>